Published OnlineFirst April 12, 2016; DOI: 10.1158/2159-8290.CD-15-1157

RESEARCH ARTICLE

Neutrophils Suppress Intraluminal NK Cell–Mediated Tumor Cell Clearance and Enhance Extravasation of Disseminated Carcinoma Cells

Asaf Spiegel[1], Mary W. Brooks[1], Samin Houshyar[1], Ferenc Reinhardt[1], Michele Ardolino[2], Evelyn Fessler[1], Michelle B. Chen[3], Jordan A. Krall[1], Jasmine DeCock[1], Ioannis K. Zervantonakis[3], Alexandre Iannello[2], Yoshiko Iwamoto[4], Virna Cortez-Retamozo[4], Roger D. Kamm[3], Mikael J. Pittet[4], David H. Raulet[2], and Robert A. Weinberg[1,5,6]

Published OnlineFirst April 12, 2016; DOI: 10.1158/2159-8290.CD-15-1157

ABSTRACT Immune cells promote the initial metastatic dissemination of carcinoma cells from primary tumors. In contrast to their well-studied functions in the initial stages of metastasis, the specific roles of immunocytes in facilitating progression through the critical later steps of the invasion–metastasis cascade remain poorly understood. Here, we define novel functions of neutrophils in promoting intraluminal survival and extravasation at sites of metastatic dissemination. We show that $CD11b^+/Ly6G^+$ neutrophils enhance metastasis formation via two distinct mechanisms. First, neutrophils inhibit natural killer cell function, which leads to a significant increase in the intraluminal survival time of tumor cells. Thereafter, neutrophils operate to facilitate extravasation of tumor cells through the secretion of IL1β and matrix metalloproteinases. These results identify neutrophils as key regulators of intraluminal survival and extravasation through their cross-talk with host cells and disseminating carcinoma cells.

SIGNIFICANCE: This study provides important insights into the systemic contributions of neutrophils to cancer metastasis by identifying how neutrophils facilitate intermediate steps of the invasion–metastasis cascade. We demonstrate that neutrophils suppress natural killer cell activity and increase extravasation of tumor cells. *Cancer Discov; 6(6); 630–49. ©2016 AACR.*

INTRODUCTION

The metastatic spread of tumor cells to distant sites is estimated to be responsible for at least 90% of cancer-related mortality, but the mechanisms leading to these secondary growths are incompletely understood. Evidence accumulated in recent years demonstrates that the invasive and metastatic traits of cancer cells are often governed by complex interactions between cancer cells and surrounding stromal cells of host origin. This cross-talk extends across multiple stages of the invasion–metastasis cascade—the sequence of events that commences with locally invasive primary tumor cells, proceeds through their intravasation, transport and survival in the circulation, extravasation into the parenchyma of distant tissues, formation of micrometastases, and finally their colonization of these tissues, yielding macroscopic metastases (1). Although the tumor-promoting effects of immune cells acting at the primary tumor site have been studied extensively (2–6), relatively little is known about how circulating immune cells affect the dynamics of the later phases of the invasion–metastasis cascade.

Among the various immune-cell populations of the host, studies of the contributions of neutrophils to cancer biology have been overshadowed by examinations of other cell types, most notably macrophages. Furthermore, the role of neutrophils in cancer has been a subject of controversy, as both tumor-promoting and tumor-suppressing effects have been reported (7–15). Neutrophils have been implicated in cancer pathogenesis because of their ability to secrete cytokines, such as IL1β, which is known to activate endothelial cells (16), and proteases, such as matrix metalloproteinases (MMP), which can cleave components of the extracellular matrix (ECM) as well as cell-surface adhesion molecules (17). In addition, MMPs can liberate growth factors that are bound in an inactive state either to the ECM or to the plasma membrane, thereby making these factors readily available to cancer cells (18, 19). Acting in these ways, MMPs have been shown to contribute to the local invasion and intravasation steps of the invasion–metastasis cascade (20–24).

Independent of the localized interactions between cancer cells and neutrophils, neutrophils can play a role in the systemic response to tumorigenesis. For example, the systemic effects of tumors on host physiology, including neutrophilia, are often observed in murine models of cancer as well as in patients with cancer (3, 5, 25–28). Moreover, elevated levels of circulating neutrophils represent a marker of poor prognosis in patients with cancer (29, 30).

In the present study, we demonstrate that the systemic effects initiated by neoplastic cells residing in the primary tumor profoundly affect their vascular intraluminal survival and extravasation at distant metastatic sites. More specifically, our results demonstrate that neutrophils, mobilized by the primary tumors, have the ability to prevent natural killer (NK) cell–mediated clearance of tumor cells from initial sites of dissemination while concurrently facilitating the extravasation of tumor cells into the lung parenchyma.

[1]Whitehead Institute for Biomedical Research, Cambridge, Massachusetts. [2]Department of Molecular and Cell Biology and Cancer Research Laboratory, Division of Immunology, University of California at Berkeley, Berkeley, California. [3]Department of Mechanical Engineering, Massachusetts Institute of Technology, Cambridge, Massachusetts. [4]Center for Systems Biology, Massachusetts General Hospital and Harvard Medical School, Boston, Massachusetts. [5]Department of Biology, Massachusetts Institute of Technology, Cambridge, Massachusetts. [6]Massachusetts Institute of Technology Ludwig Center for Molecular Oncology, Cambridge, Massachusetts.

Note: Supplementary data for this article are available at Cancer Discovery Online (http://cancerdiscovery.aacrjournals.org/).

Current address for E. Fessler: Laboratory for Experimental Oncology and Radiobiology, Center for Experimental Molecular Medicine, Academic Medical Center, University of Amsterdam, Amsterdam, the Netherlands.

Corresponding Author: Robert A. Weinberg, Whitehead Institute for Biomedical Research, 9 Cambridge Center, Cambridge, MA 02142. Phone: 617-258-5159; Fax: 617-258-5213; E-mail: weinberg@wi.mit.edu

doi: 10.1158/2159-8290.CD-15-1157

Published OnlineFirst April 12, 2016; DOI: 10.1158/2159-8290.CD-15-1157

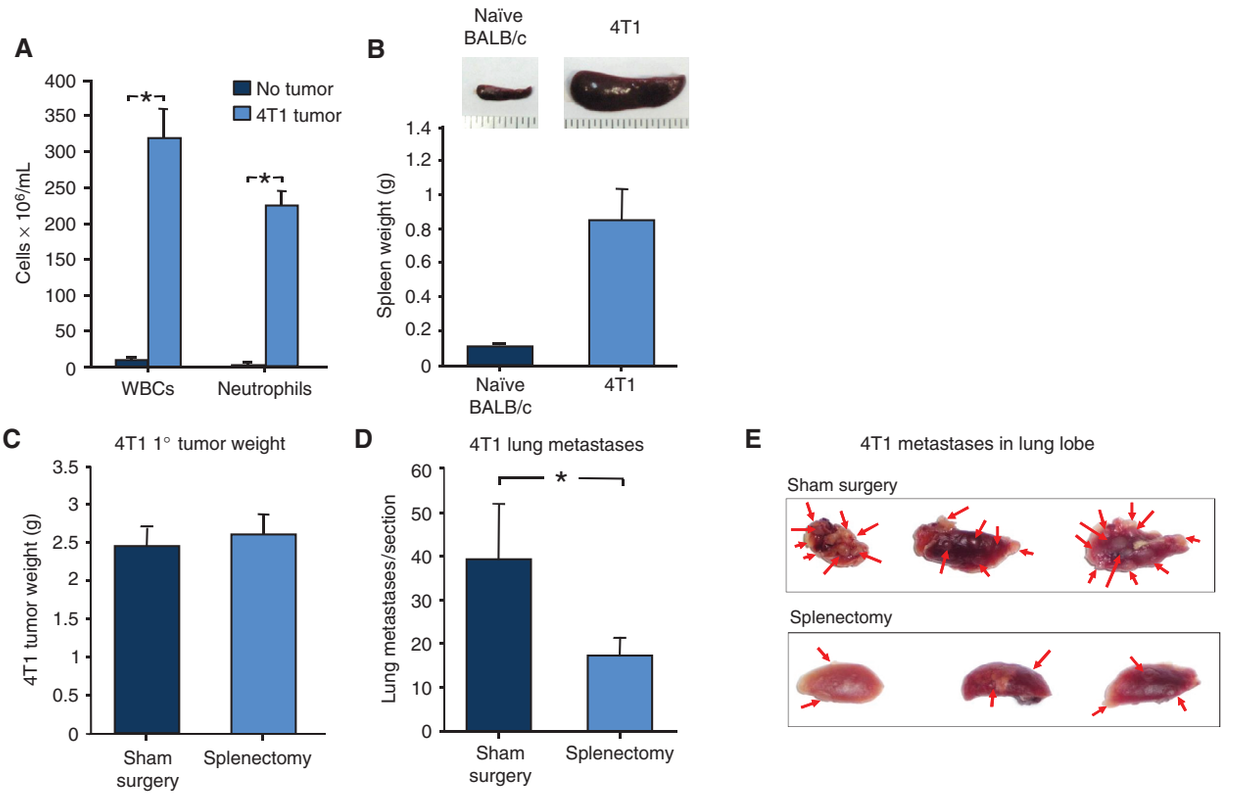

Figure 1. Tumor metastasis is mediated by neutrophils. **A,** total leukocyte (WBC) and neutrophil counts in blood from control noninjected mice or 4 to 5 weeks after implantation with murine mammary carcinoma 4T1 cells. $n \geq 9$ mice for each group. **B,** representative picture (top) and average weight (bottom) of spleen from naïve BALB/c (control) or 5 weeks after s.c. implantation of mice with 4T1 cells. $n \geq 8$ mice for each group. **C,** 4T1 tumor weight in sham-operated BALB/c mice (control) or splenectomized mice. $n \geq 17$ for each group. **D,** number of 4T1 lung metastases (per hematoxylin and eosin–stained section comprising all five lobes) in mice implanted with 4T1 cells in sham-operated BALB/c mice (control) or splenectomized mice. $n \geq 12$ for each group. **E,** representative picture of lung lobes from sham surgery or splenectomized mice. Red arrows point to lung metastases. (*continued on following page*)

RESULTS

Tumor Metastasis Is Facilitated by Neutrophils

In order to study systemic mechanisms that facilitate tumor progression, we used an established *in vivo* experimental system using the previously described murine mammary carcinoma 4T1 cells (31, 32). When injected subcutaneously (s.c.) into syngeneic BALB/c hosts, 4T1 cells form vigorously growing primary tumors and are able to complete all steps of the metastatic cascade, resulting in the formation of large numbers of visible metastatic nodules in the lungs (31). We confirmed earlier reports using the 4T1 tumor model (12–14, 33), and observed a 100-fold elevation in the number of circulating white blood cells (WBC) in 4T1 tumor–bearing mice (hereafter termed 4T1 mice; 4 weeks after implantation) relative to normal control hosts; neutrophils accounted largely for this expansion of the WBC compartment (Fig. 1A). Of note, implantation of 4T1 tumors either orthotopically or subcutaneously yielded similar effects in terms of neutrophilia as well as splenomegaly (Supplementary Fig. S1A). Accordingly, we proceeded with s.c. implantation of 4T1 cells, because this method eliminates the significant immune effects that result from the far more invasive orthotopic surgery and postsurgical wound healing.

ELISA analysis demonstrated that cultured 4T1 cells secreted high levels of G-CSF (1.14 ± 0.35 ng/mL/10^6 cells), a cytokine that has been shown to cause the expansion and mobilization of neutrophils (12). Furthermore, given that the expression of the G-CSF receptor was undetectable in this tumor cell line (Supplementary Fig. S1B), it was unlikely that the secreted G-CSF acted in an autocrine manner. Hence, the 4T1 tumor model and its associated neutrophilia provided the necessary platform to study the role of neutrophils in cancer progression.

We also noted a 10-fold increase in spleen weight of 4T1 mice (Fig. 1B) and wished to determine whether this splenomegaly contributed in any way to the metastatic ability of the 4T1 cells, because the spleen can serve as an important reservoir of myeloid cells such as neutrophils (34). To test this notion, we removed the spleens of BALB/c mice prior to implanting 4T1 tumor cells s.c. We chose splenectomy because postsurgical recovery is rapid and there are few systemic side effects on host physiology. In splenectomized mice relative to nonsplenectomized 4T1 mice, we observed a 50% reduction in the total number of circulating WBCs, which was paralleled

Published OnlineFirst April 12, 2016; DOI: 10.1158/2159-8290.CD-15-1157

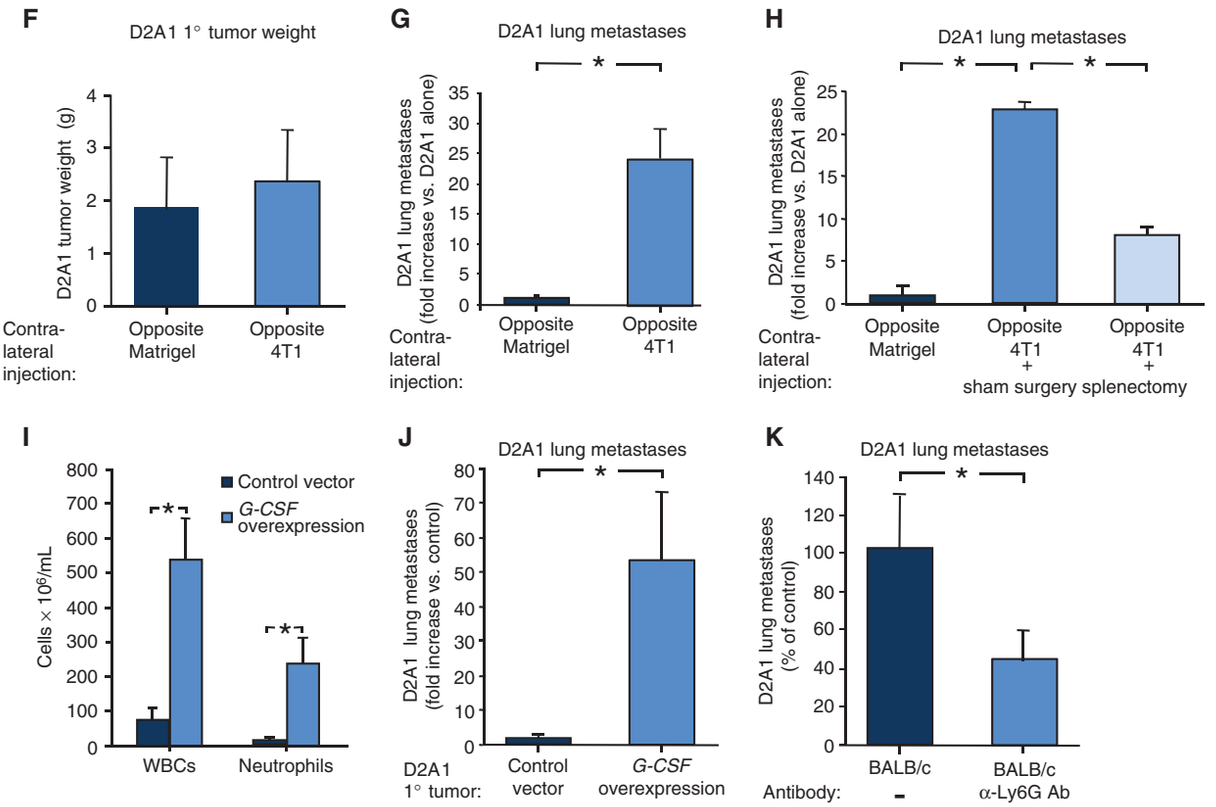

Figure 1. ***(Continued)*** **F,** D2A1 primary tumor weight 4 to 5 weeks after s.c. implantation of mice with D2A1 cells contralateral to 4T1 cells or Matrigel (control). $n \geq 19$ for each group. **G,** D2A1 lung metastases (fold increase vs. D2A1 injected contralaterally to Matrigel) in mice implanted with D2A1 cells contralateral to 4T1 cells or Matrigel (control). $n \geq 14$ for each group. **H,** D2A1 lung metastases (fold increase vs. D2A1 injected contralaterally to Matrigel) in sham-operated or splenectomized mice implanted with D2A1 cells contralateral to 4T1 cells. $n \geq 8$ for each group. **I,** total leukocyte (WBC) and neutrophil counts in blood from mice 4 to 5 weeks after implantation with D2A1 cells ectopically expressing empty vector (control) or *G-CSF*. $n \geq 9$ mice for each group. **J,** D2A1 lung metastases spontaneously arising in mice bearing primary tumors of D2A1 cells ectopically expressing *G-CSF* or empty vector (control). $n \geq 7$ for each group. **K,** number of D2A1 metastases in lungs of mice lacking primary tumors 2 weeks after i.v. injection of D2A-Tom$^+$ cells. Mice were injected with PBS, or anti-Ly6G antibody 24 hours before i.v. injection of cells. $n \geq 7$ for each group. *, $P < 0.05$.

by a similar reduction in the number of neutrophils at the time the experiments were terminated (4–5 weeks after 4T1 cell implantation; Supplementary Fig. S1C). Although there was no reduction in the weights of primary tumors in splenectomized mice (Fig. 1C), splenectomy prior to s.c. injection of 4T1 tumor cells led to a 56% reduction in the number of pulmonary metastases formed relative to those in the control, sham-operated mice (Fig. 1D and E).

We wished to further verify that the efficient metastasis of 4T1 tumor cells depended in significant part on systemic physiologic effects. To address this possibility, we asked whether implantation of 4T1 tumors would affect the spontaneous metastasis of D2A1 murine mammary carcinoma cells implanted s.c. on the contralateral flank of a syngeneic host BALB/c mouse. When implanted on their own, D2A1 primary tumors rarely spawn pulmonary metastases (35). However, D2A1 cells are able to form macroscopic metastases in the lung when injected in large numbers intravenously (36). (Of note, the number of neutrophils in D2A1 tumors was 5-fold lower than that found in 4T1 tumors: 1,634 ± 318/g of tumor and 8,127 ± 1762/g of tumor, respectively.)

Although no significant change in D2A1 primary tumor weight was noted in response to contralateral implantation of 4T1 cells (Fig. 1F), a 22-fold increase in the number of D2A1-derived lung metastases was observed relative to D2A1 tumors implanted contralaterally to control Matrigel implants (Fig. 1G). These results indicated that 4T1 cells could create a systemic environment that enabled metastasis of otherwise nonmetastatic or weakly metastatic carcinoma cells. We mention in passing that the contralateral implantation of D2A1 cells did not affect the number of 4T1 metastatic lesions. Importantly, splenectomy substantially reduced the ability of 4T1 tumors to induce the metastasis of contralaterally implanted D2A1 tumors, as evidenced by a 67% decrease in D2A1 pulmonary metastases (Fig. 1H). Hence, optimal expression of the systemic effects wrought by 4T1 cells depended on an intact spleen, which ostensibly served as a reservoir for myeloid cells mediating these effects.

We proceeded to express *G-CSF* in D2A1 cells, which do not on their own ordinarily express this cytokine. G-CSF overexpression in D2A1 cells (secreted levels were comparable and even slightly higher than 4T1 cells; Supplementary Fig. S1D)

Published OnlineFirst April 12, 2016; DOI: 10.1158/2159-8290.CD-15-1157

was able to phenocopy the systemic neutrophilia provoked by 4T1 tumors (Fig. 1I) and yielded a 54-fold increase of D2A1 metastases formed in the lungs (Fig. 1J). Collectively, these experiments demonstrated that the G-CSF–driven expansion of neutrophils is both necessary and sufficient for this response.

Although the mechanism of the systemic potentiation of metastasis was still undefined at this point, its effects on D2A1 cells were transient and reversible. Thus, when we isolated D2A1 tumor cells that had successfully metastasized to the lungs of contralaterally implanted 4T1 mice and reinjected these cells into naïve mice, the previously metastasized D2A1 cells were no more able, on a per-cell basis, to metastasize than parental cells that had not experienced the systemic environment present in a 4T1-bearing host (data not shown).

These results pointed to an important role for neutrophils in driving metastasis. To further explore the contribution of neutrophils to this process, we asked whether normal, physiologic levels of neutrophils, rather than the dramatic neutrophilia observed in 4T1-bearing hosts, might also function to promote tumor metastasis. To address this question, we depleted neutrophils in non–tumor-bearing mice by injecting the 1A8 monoclonal antibody, which depletes specifically Ly6G$^+$ neutrophils but not granulocyte receptor-1$^+$ (Gr1$^+$) monocytes (37). This depletion of neutrophils prior to intravenous (i.v.) injection (a route that allows them to form metastatic lesions, as cited earlier) of D2A1 cells led to a 56% decrease in metastases in the lungs of these animals (Fig. 1K). Thus, even normal, physiologic levels of circulating neutrophils could indeed promote metastasis, and enhancing these levels could serve as a useful experimental tool to better understand the role of immune cells in tumor metastasis. Furthermore, the results of this experiment suggested that neutrophils might primarily affect postintravasation processes, an issue that we address in more detail below.

Neutrophils Facilitate Intermediate Steps of the Invasion–Metastasis Cascade

Responding to the above-described results, we attempted to delineate the specific steps of the invasion–metastasis cascade that were affected by the neutrophils. To address whether mobilized neutrophils might infiltrate the primary tumor and affect cells within these growths, D2A1 cells were co-mixed with splenocytes from 4T1-bearing mice and coinjected s.c. into BALB/c mice. No metastatic D2A1 nodules were observed in these mice, indicating that direct heterotypic interactions between the splenocytes and the tumor cells within the primary tumor were unlikely to be responsible for the observed increased metastasis (data not shown).

We next tested whether the systemic environment in 4T1 mice affected the ability of D2A1 tumor cells to intravasate. When D2A1 cells were implanted contralaterally to 4T1 tumors, only a marginal (2-fold) increase was observed in the number of circulating D2A1 tumor cells 4 to 5 weeks after implantation of the primary tumors (relative to control mice in which D2A1 cells had been implanted contralaterally to Matrigel plugs; Supplementary Fig. S2A). These results suggested that the >20-fold increase in D2A1 metastasis triggered by distant 4T1 primary tumors (Fig. 1H) was not likely to result from differences in the ability of D2A1 primary tumor cells to intravasate at increased rates in the presence of the distant 4T1 tumors.

Collectively, the above experiments suggested that the metastasis-promoting role of neutrophils acts on the post-intravasation steps of the invasion–metastasis cascade. To directly test this notion, we asked whether the systemic environment of a 4T1-bearing host would promote the metastasis of i.v. injected D2A1 cells that have bypassed the early steps of invasion and intravasation because of their route of introduction into mice. We injected a relatively small number of D2A1 cells (2×10^4), as this size of inoculum more closely mimics conditions of spontaneous metastasis. Under these conditions, we found that mice bearing already-established s.c. 4T1 tumors experienced a 12-fold increase in the number of D2A1 lung foci relative to naïve mice.

We extended these analyses to both MDA-MB-231 human breast cancer cells and B16-F10 mouse melanoma cells (both injected into immune-deficient NOD/SCID mice) and observed similarly strong metastasis promotion in 4T1-bearing mice (Fig. 2A) upon i.v. injection of 2×10^4 cells. These results provided direct evidence that the previously observed systemic effects of primary 4T1 tumors could be ascribed largely, if not entirely, to facilitation of the later (i.e., post-intravasation) steps of the invasion–metastasis cascade.

We reasoned that the observed metastasis-promoting effects of established 4T1 primary tumors on i.v. injected tumor cells could result from two alternative mechanisms: (i) tumor cells disseminated by the 4T1 primary tumors reached the lungs earlier than the D2A1 cells and persisted in this tissue, thereby creating a favorable pulmonary microenvironment for subsequent metastasis formation by D2A1 cells; or (ii) the G-CSF released by 4T1 cells induced mobilization of neutrophils that facilitate the metastasis of D2A1 cells.

To address the first possibility, we injected 2×10^4 4T1 cells i.v., 1 day before injection of D2A1 cells. However, no increase in the number of D2A1 metastases formed was detected under these conditions (Supplementary Fig. S2B), eliminating direct interactions between 4T1 and D2A1 cells in the lungs as a cause for the increased metastasis of D2A1 cells in 4T1-bearing mice.

Wishing to critically test the second hypothesized mechanism, we determined whether the splenocytes induced by 4T1 primary tumors sufficed, on their own, to increase the metastasis of D2A1 cells. We therefore performed adoptive transfer of splenocytes isolated from 4T1-bearing mice into naïve, non–tumor-bearing mice. One hour after the introduction of these splenocytes, D2A1 cells were injected i.v. into these mice. As depicted in Fig. 2B, adoptive transfer of splenocytes prior to i.v. injection of D2A1 cells led to a 6.6-fold increase in eventual metastasis formation by D2A1 cells.

Taken together, these results indicated that the observed increase in metastasis elicited by 4T1 tumors was mediated primarily, and possibly entirely, by 4T1-mobilized neutrophils that could, on their own, drive enhanced metastasis formation. Conversely, a significant contribution of disseminated 4T1 carcinoma cells that had arrived previously in the

Published OnlineFirst April 12, 2016; DOI: 10.1158/2159-8290.CD-15-1157

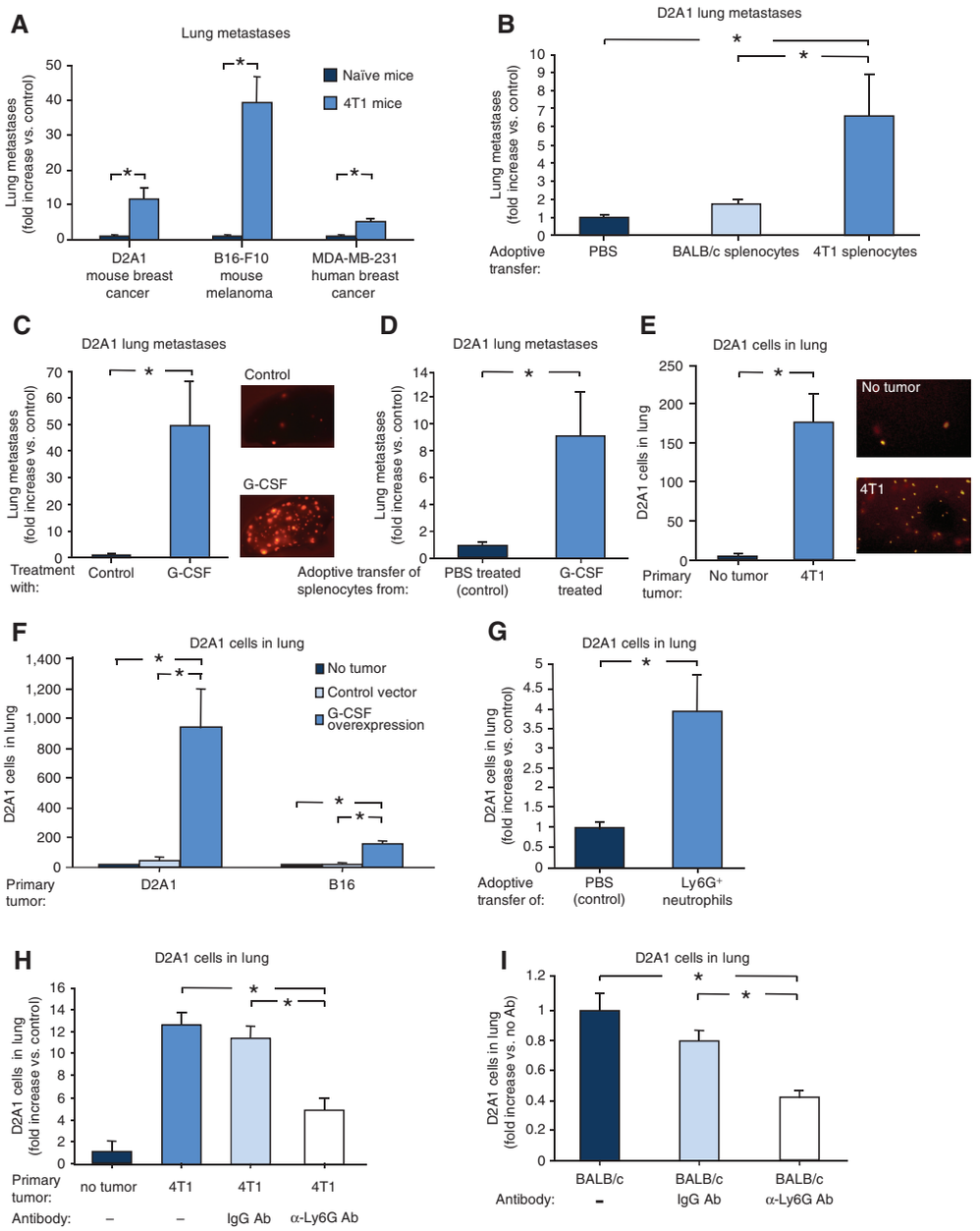

Figure 2. Neutrophils facilitate intermediate steps of the invasion–metastasis cascade. **A,** lung metastasis (non-4T1) in mice injected i.v. with 2×10^4 D2A1-Tom$^+$, B16-F10-GFP$^+$, or MDA-MB-231-Tom$^+$ cells. Results show fold increase upon injection into 4T1 tumor–bearing mice versus naive non–tumor-bearing mice (control). B16-F10-GFP$^+$ and MDA-MB-231-Tom$^+$ cells were injected into NOD/SCID 4T1 tumor–bearing mice 14 days after implantation of 4T1 cells. The experiment was terminated 2 to 3 weeks later, and lung metastases were quantified. $n \geq 8$ for each group. **B,** D2A1 lung metastases in mice (fold increase vs. control PBS injection) following adoptive transfer of splenocytes from non–tumor-bearing or 4T1 tumor–bearing mice. $n \geq 9$ for each group. **C,** number of D2A1-Tom$^+$ metastases in lungs of G-CSF–treated mice compared to control (PBS-treated) mice. $n \geq 13$ for each group. **D,** number of D2A1-Tom$^+$ metastases in lungs following adoptive transfer of splenocytes from G-CSF–treated mice (fold increase compared to control mice that were injected with splenocytes from PBS-treated mice). $n \geq 12$ for each group. **E,** number of D2A1-Tom$^+$ cells in lungs of 4T1 (or naïve control) mice 24 hours after i.v. injection of D2A1 cells (left). Representative lung lobe images (right). The 4T1 mice had been implanted with 4T1 cells 4 weeks earlier. **F,** number of D2A1-Tom$^+$ cells in lungs of mice after i.v. injection of D2A1-Tom$^+$ cells into either control naïve mice, or mice bearing primary tumors of D2A1 or B16-F10 cells ectopically expressing G-CSF (implanted 4 weeks earlier). $n \geq 6$ for each group. **G,** number of D2A1-Tom$^+$ cells in lungs of mice (fold increase vs. control PBS injection) following adoptive transfer of Ly6G$^+$-enriched neutrophils from splenocytes from 4T1 tumor–bearing mice. $n \geq 7$ for each group. **H,** D2A1-Tom$^+$ cells in lungs (fold increase compared to control mice without primary tumors) of 4T1 mice 24 hours after i.v. injection of D2A1 cells. Mice were injected with PBS, IgG antibody or anti-Ly6G (1A8) antibody 24 hours before injection of cells. Non–tumor-bearing mice served as a control. $n \geq 10$ mice per group. **I,** number of D2A1-Tom$^+$ cells in lungs of non–tumor-bearing mice 24 hours after i.v. injection of D2A1 cells. Mice were injected with PBS, control IgG antibody, or anti-Ly6G antibody 24 hours before i.v. injection of cells. $n \geq 11$ for each group. For **B–D,** the experiment was terminated and D2A1 lung metastases were quantified 2 weeks after i.v. injection of D2A1 cells. For **E–I,** the experiment was terminated 24 hours after i.v. injection of D2A1 cells, and the number of D2A1-Tom$^+$ cells in the lung was assessed. In adoptive transfer experiments (**B** and **G**), splenocytes were obtained from 4T1 mice that had been implanted with 4T1 cells 4 weeks earlier. *, $P < 0.05$.

Published OnlineFirst April 12, 2016; DOI: 10.1158/2159-8290.CD-15-1157

lungs and created a "niche" for subsequently arriving D2A1 cells was ruled out.

Localization of the effects of 4T1 tumors to the later steps of the invasion–metastasis cascade allowed us to further resolve the effects of G-CSF. Thus, treating mice with 5 daily injections of G-CSF prior to the i.v. injection of D2A1 cells resulted in a 48-fold increase in the number of D2A1 lung metastases (Fig. 2C). Hence, subcutaneously introduced G-CSF could essentially phenocopy the effects of 4T1 primary tumors.

Wishing to ensure that G-CSF acts via the mobilization of neutrophils rather than by alternative mechanisms, we repeated the above experiment using the adoptive transfer of splenocytes from tumor-free mice that had been treated with G-CSF (5 daily injections). The number of D2A1 pulmonary metastases was 9-fold higher in recipients of splenocytes from these G-CSF-treated mice relative to injection of the same number of splenocytes from control PBS-treated mice (Fig. 2D). Hence, these effects in enhancing metastasis formation operated after the entrance of the immune cells into the general circulation and once again appeared to be confined to the later stages of the invasion–metastasis cascade. Moreover, this effect could be achieved by cells that accumulated in large numbers in the spleens following systemic G-CSF treatment.

We addressed postextravasation effects of 4T1-induced splenocytes by examining the effects of circulating immune cells on colonization, i.e., the outgrowth of micrometastases in the lung parenchyma into macroscopic deposits. Thus, we injected D2A1 cells i.v. into naïve mice and allowed them 48 hours to extravasate, thereby enabling us to focus solely on postextravasation events. We note that D2A1 cells extravasate less than 48 hours after entering the circulation (38). When we thereafter injected splenocytes from 4T1-bearing mice into these mice, we observed no increase in the number of lung macrometastases formed by the previously extravasated D2A1 cells relative to control mice that had not been treated with adoptive transfer of splenocytes (Supplementary Fig. S2C). These observations, when taken together, indicated that the G-CSF–induced neutrophils acted to foster metastasis after intravasation but before postextravasation colonization.

Neutrophils Increase Accumulation of Cancer Cells in the Lungs

We attempted to delineate with even more precision the specific postintravasation steps of metastasis that were facilitated by neutrophils. When comparing survival of D2A1 tumor cells in control and 4T1-bearing hosts, we found that 24 hours after i.v. injection of D2A1 cells, the number of these cells that were present in the lungs of 4T1 primary tumor-bearing mice was greatly increased (50-fold) compared to the D2A1 cells detected in naïve hosts (Fig. 2E). We further tested whether primary tumors derived from either D2A1 or B16-F10 cells, engineered in both cases to express ectopic G-CSF, would be able to promote retention of D2A1 cells in the lungs after i.v. injection. As mentioned above (Supplementary Fig. S1D) for D2A1 cells, this forced expression of G-CSF in B16-F10 cells resulted in secreted levels of this cytokine that were comparable to those secreted by 4T1 cells (Supplementary Fig. S2D). The number of D2A1 cells retained in the lungs was increased 20-fold in mice bearing D2A1–G-CSF primary tumors and 11-fold in mice bearing B16-F10–G-CSF primary tumors relative to corresponding control tumors that did not secrete this cytokine (Fig. 2F). Hence, in both cases, the forced expression of *G-CSF* resulted in greatly increased retention of disseminated cells within the lungs.

We proceeded to assess a specific role for neutrophils in mediating tumor cell retention in the lung. In fact, the spleens of 4T1 mice are populated by heterogeneous populations of cells. In order to test for the specific involvement of neutrophils, we conducted adoptive transfer experiments in which Ly6G$^+$-enriched neutrophils were injected into naïve, non–tumor-bearing mice. One hour after introduction of the neutrophils, D2A1 cells were injected i.v. into these mice. This led to a 3.5-fold increase in the number of D2A1 cells retained in the lung (Fig. 2G).

We further verified that tumor cell retention in the lungs was mediated specifically by neutrophils by treating 4T1 tumor–bearing mice with the neutrophil-depleting 1A8 antibody. This resulted in a 54% reduction in the number of D2A1 cells found in the lungs of 4T1 mice 24 hours after i.v. injection, relative to untreated or IgG-treated controls (Fig. 2H). Furthermore, physiologic levels of neutrophils present in naïve, non–tumor-bearing mice were also important in facilitating retention of i.v.-injected tumor cells, as evidenced by the fact that depletion of these neutrophils (using anti-Ly6G antibodies) resulted 24 hours later in a 58% reduction (relative to untreated or IgG-treated controls) in the number of i.v.-injected D2A1 cells found in the lungs of mice (Fig. 2I). Hence, even the normally present circulating neutrophils are intrinsically capable of facilitating metastasis by increasing the accumulation of tumor cells in the lungs within the short time period after introduction of the tumor cells into the venous circulation.

Neutrophils Inhibit NK Cell–Mediated Clearance of Tumor Cells

The observed increased accumulation of carcinoma cells in the lungs was compatible, in principle, with three alternative neutrophil-mediated mechanisms: more efficient physical trapping of intravasated carcinoma cells in the lung microvessels, enhanced intraluminal survival of intravasated cells, or elevated extravasation of these cells. Accordingly, we explored the trapping of D2A1 cells in the lung capillary beds using *in vivo* bioluminescent measurements conducted 10 minutes after i.v. injection; in this instance, we found no significant differences in the numbers of D2A1 cells found in the lungs of naïve mice or 4T1-bearing mice. This indicated that initial physical trapping of cells in pulmonary microvessels was not affected by the presence of splenocytes (Fig. 3A and B).

A significant difference in the number of D2A1 cells in the lungs was apparent, however, soon after this initial trapping. Thus, 70% of D2A1 cells injected into naïve mice had been cleared from the lungs within 4 hours after i.v. injection (Fig. 3A and B). In contrast, in mice bearing 4T1 primary tumors, only 20% of the D2A1 cells were cleared from the lungs of 4T1 mice by this time. These results suggested that the systemic changes in mice bearing 4T1 primary tumors acted to reduce the otherwise-rapid attrition of D2A1 cells initially trapped in the lungs (Fig. 3B).

Published OnlineFirst April 12, 2016; DOI: 10.1158/2159-8290.CD-15-1157

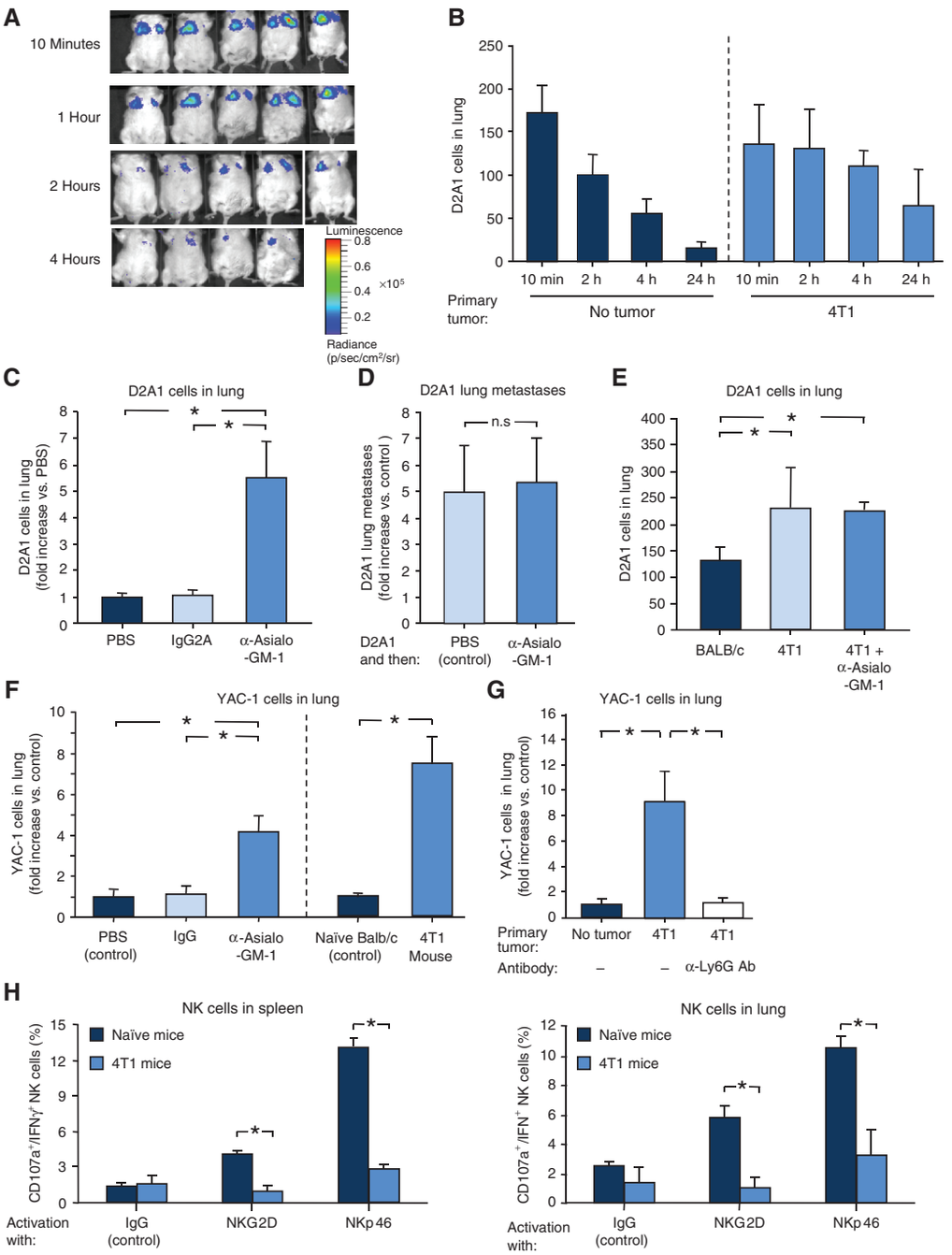

Figure 3. Neutrophils inhibit NK cell–mediated clearance of tumor cells. **A,** representative bioluminescent imaging of BALB/c mice injected with D2A1-Tom$^+$ cells expressing luciferase. **B,** number of D2A1-Tom$^+$ cells detected in large lobes of lungs at the indicated time points after i.v. injection of D2A1-Tom$^+$ cells into control naïve mice or 4T1 mice (implanted with 4T1 cells 4 weeks earlier). $n \geq 6$ for each time point. **C,** number of D2A1-Tom$^+$ cells in lungs of mice 4 hours after i.v. injection of D2A1-Tom$^+$ cells. Mice were injected with PBS (control), IgG2A antibody, or anti–asialo-GM-1 antibody 24 hours before injection of cells. Results show fold increase versus control non–tumor-bearing mice. $n \geq 8$ for each group. **D,** D2A1-Tom$^+$ lung metastases in mice (fold increase vs. control PBS-treated mice) following injection of anti–asialo-GM-1 antibody 24 hours after injection of cells. $n \geq 5$ for each group. **E,** number of D2A1-Tom$^+$ cells detected in lungs 4 hours after i.v. injection into control non–tumor-bearing mice, 4T1-bearing mice, or 4T1-bearing mice that had been injected with anti–asialo-GM-1 antibody 24 hours before injection of cells. $n \geq 6$ for each group. **F** (left), number of YAC-1 cells in lungs of non–tumor-bearing BALB/c mice 4 hours post i.v. injection of YAC-1 cells. Mice were injected with PBS (control), IgG2A antibody, or anti–asialo-GM-1 antibody 24 hours before injection of cells. $n \geq 8$ for each group. Right, number of YAC-1 cells detected in lungs 4 hours after i.v. injection into control non–tumor-bearing mice or 4T1-bearing mice. $n \geq 6$ for each group. **G,** YAC-1 cells in lungs (fold increase compared to control mice without primary tumors) of 4T1 mice 4 hours after i.v. injection of YAC-1 cells. Mice were injected with PBS or anti-Ly6G (1A8) antibody 24 hours before injection of cells. $n \geq 8$ for each group. **H,** percentage of IFNγ$^+$/CD107a$^+$ NK cells from the spleens (left) and lungs (right) of 4T1 tumor–bearing or non–tumor-bearing naïve mice following *in vitro* stimulation of the cells with NK cell–activating receptor antibodies or IgG control. $n \geq 6$ for each group. In **B, F, G,** and **H,** host 4T1 mice had been implanted with 4T1 cells 4 weeks earlier. *, $P < 0.05$.

Published OnlineFirst April 12, 2016; DOI: 10.1158/2159-8290.CD-15-1157

We hypothesized that the neutrophils might protect cancer cells from rapid intraluminal clearance from pulmonary microvessels by inhibiting the NK cells, which are normally responsible for this function (39, 40). By depleting NK cells in BALB/c mice using the anti–asialo-GM-1 antibody (41), we determined that NK cells do, in fact, clear D2A1 cells from the circulation. Thus, ablation of NK cells prior to injection of D2A1 cells resulted in a 5.5-fold increase in the number of D2A1 cells found in the lung 4 hours after i.v. injection of these tumor cells (Fig. 3C).

Similarly, depletion of NK cells in a C57BL/6 background using the strain-specific antibody NK1.1 resulted in a 7-fold increase in the number of B16-F10 melanoma cells found in the lung 4 hours after i.v. injection of the tumor cells (Supplementary Fig. S3). These observations indicated that NK cells play a major role in preventing tumor cell accumulation in the lungs, ostensibly by reducing the intraluminal survival time of the tumor cells. Importantly, when NK cells were depleted 24 hours after injection of D2A1 cells—a time when tumor cells have either extravasated or been cleared from the vasculature—no increase in lung metastases was observed (Fig. 3D), indicating that NK cells acted while cancer cells still resided within the lumina of microvessels, not thereafter.

We wished to further validate that the increased survival of intraluminal D2A1 cells promoted by neutrophils in 4T1-bearing hosts was due to protection of these cells from NK cell–mediated clearance and not by some other neutrophil-induced, NK cell–independent mechanism. To distinguish between these possibilities, we depleted NK cells from 4T1 mice (by treating with anti–asialo-GM1) prior to i.v. injection of D2A1 cells. As depicted in Fig. 3E, this antibody treatment did not result in further reduction of D2A1 cell clearance beyond the reduction observed in 4T1 mice that had not been depleted of NK cells. Accordingly, the ability of NK cells to kill the intraluminal tumor cells was already significantly impaired in 4T1 mice in a manner that could not be further reduced by the NK cell–depleting antibody.

Yet, other observations provided further support for the notion that neutrophils protect cancer cells in intraluminal sites from NK cell–mediated clearance. To explore this further, we made use of YAC-1 cells, which are established targets of NK cell–mediated clearance (42), and indeed found that YAC-1 clearance was NK cell–dependent, because depletion of NK cells using anti–asialo-GM-1 antibodies resulted in a 4.5-fold increase in the number of YAC-1 cells found in the lung 4 hours after i.v. injection (Fig. 3F). Moreover, the clearance of YAC-1 cells was inhibited when injected into 4T1-bearing mice relative to control mice (Fig. 3F). Importantly, consistent with our results with D2A1 cells (Fig. 2G), the protection of YAC-1 cells from NK cell–mediated clearance in 4T1-bearing mice was dependent upon neutrophils, as neutrophil depletion abrogated any protective effects in these mice (Fig. 3G). These observations, when taken together, allowed us to conclude that neutrophils mobilized in 4T1-bearing mice protect tumor cells from NK cell–mediated clearance, thereby prolonging their survival in the circulation and increasing the number of cells that could, in principle, subsequently form metastases.

We also undertook to further characterize the mechanism by which neutrophils inhibited the NK cell–mediated clearance of circulating D2A1 cells. The observed differences in NK-cell activity between 4T1 mice and control non–tumor-bearing hosts did not result from a reduction in the numbers of circulating NK cells, as we detected similar numbers of NK cells in the lungs of both groups of mice. This strongly suggested that the reduced NK cell–mediated clearance resulted from a decrease in the functionality of individual NK cells.

To address this possibility, we used a commonly used measure to gauge NK cell function by examining NK cell responsiveness *ex vivo*. This was assayed by functional activation of NK cells obtained from the lungs and spleens of 4T1 tumor–bearing mice and from control naïve mice. Thus, we used plate-bound antibodies specific for the NKG2D or NKp46 NK cell–activating receptors, or control IgG, followed by flow cytometry to assess intracellular IFNγ production and degranulation (indicated by CD107a expression; refs. 43, 44). As depicted in Fig. 3H, 5% of the NK cells of control naïve mice were $CD107a^+/IFN\gamma^+$ in response to NKG2D stimulation, and 10% to 12% of the NK cells were $CD107a^+/IFN\gamma^+$ in response to NKp46 stimulation. In contrast, in NK cells obtained from spleens or lungs of 4T1 mice, a >3-fold reduction in the percentage of cells that were responsive to receptor stimulation was observed; <1.5% of NK cells were $CD107a^+/IFN\gamma^+$ in response to NKG2D stimulation (similar to baseline levels obtained from stimulation with IgG control), and <4% of the NK cells were $CD107a^+/IFN\gamma^+$ in response to NKp46 stimulation (Fig. 3H). Together with earlier data, these results argued that the unique systemic response provoked by 4T1 tumors, namely, the expansion and mobilization of neutrophils, led in turn to inhibition of the ability of NK cells to undergo functional activation and thereby attenuated the NK cell–mediated clearance of intraluminal tumor cells.

Neutrophils Promote Extravasation of Intraluminal Tumor Cells

Extravasation is a crucial step in metastasis formation (45). Having confined the effects of neutrophils on metastasis to stages after intravasation and prior to colonization of the lung parenchyma, we considered whether neutrophils might facilitate extravasation of tumor cells from the lumina of pulmonary microvessels. We had previously observed that neutrophils increase the number of D2A1 cells surviving in the lungs 24 hours after their i.v. injection (Fig. 2G), but the proportion of extravasated carcinoma cells relative to those retained within the lumina of microvessels remained unknown. To examine this in more detail, we injected human breast cancer cells (MDA-MB-231) i.v. into NOD/SCID mice. Two hours later, we i.v. injected a human-specific HLA-A2 antibody that binds to class I MHC displayed by MDA-MB-231 cells. This protocol enabled us to label only cells of human origin, and only those present in the vascular lumen, but not breast cancer cells that had already extravasated.

Two hours after their injection, 70% of the MDA-MB-231 cells that were still present in the lungs of 4T1 mice were unstained by the antibody, suggesting that they had already extravasated from intraluminal sites and had therefore invaded the lung parenchyma. In contrast, only 30% of cancer cells retained in the lungs of the naïve mice had, as gauged by lack of antibody staining, escaped from the lumina and arrived in the parenchyma (Fig. 4A). This indicated that

Published OnlineFirst April 12, 2016; DOI: 10.1158/2159-8290.CD-15-1157

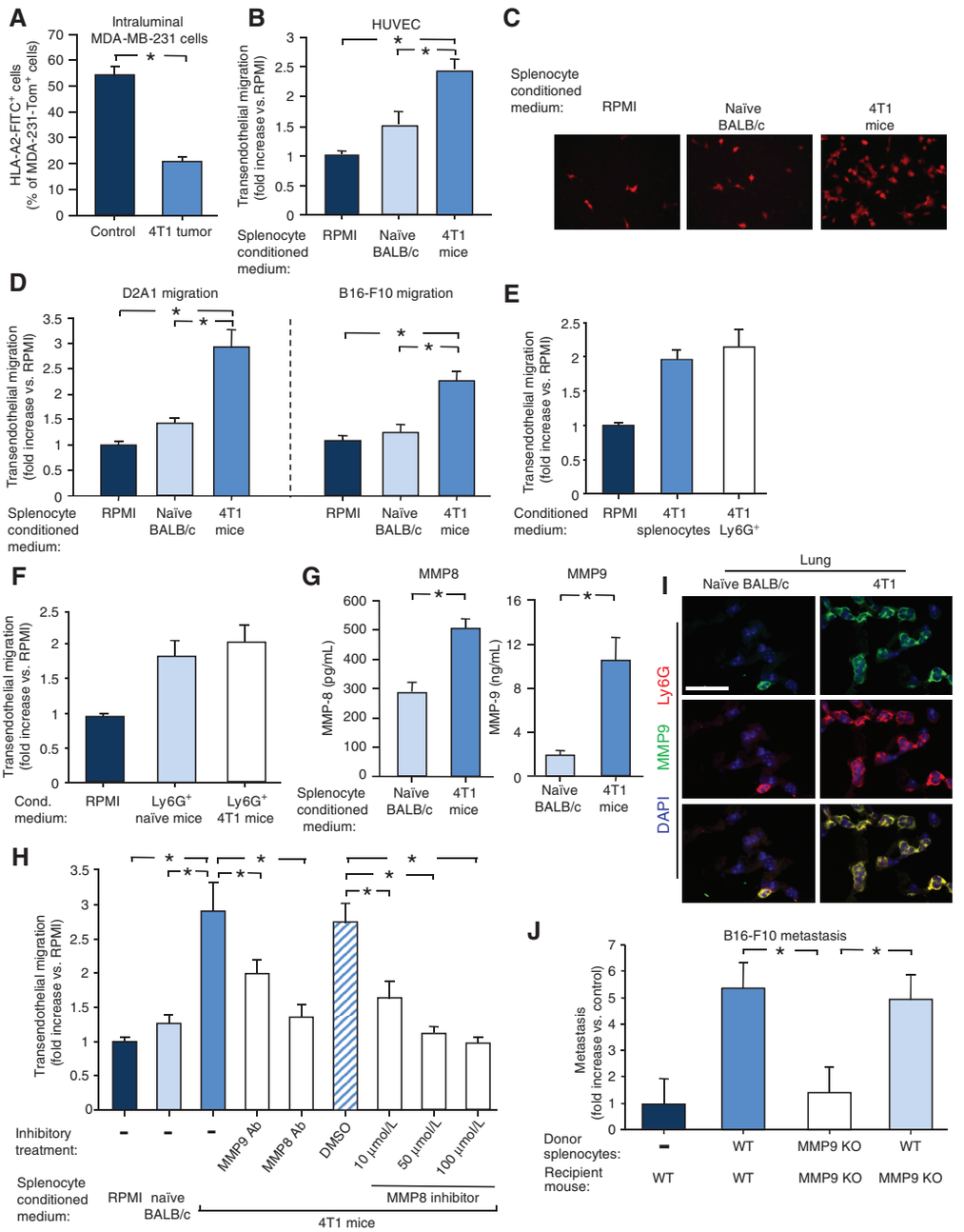

Figure 4. MMP8 and MMP9 facilitate transendothelial migration and metastasis. **A,** intraluminal antibody staining of MDA-MB-231 cells injected i.v. into 4T1 mice (implanted with 4T1 cells 4 weeks earlier) or control naïve mice. Graph shows the percentage of MDA-MB-231-Tom$^+$ cells found in the lung that also stained positive by i.v.-injected anti–HLA-2-FITC antibodies. $n \geq 6$ for each group. **B,** transendothelial migration of D2A1-Tom$^+$ cells through human umbilical vein endothelial cells (HUVEC) in the presence of the indicated conditioned media. Results present fold increase compared to control RPMI medium. At least 3 experiments were performed in duplicate. **C,** representative images of D2A1-Tom$^+$ cells that migrated through HUVECs in the presence of the indicated conditioned media. **D,** transendothelial migration of D2A1-Tom$^+$ cells or B16-F10-GFP$^+$ cells through mouse endothelial bEnd.3 cells in the presence of the indicated conditioned media. Results present fold increase compared to control RPMI medium. At least 3 experiments were performed in duplicate. **E,** transendothelial migration of D2A1 cells (fold increase compared to control RPMI medium) through mouse endothelial bEnd.3 cells in the presence of conditioned medium from unfractionated splenocytes or the Ly6G$^+$ enriched subpopulation of splenocytes from 4T1 mice. The number of Ly6G$^+$ cells used to prepare the conditioned medium was equivalent to the number of Ly6G$^+$ cells in 1.5×10^7 unfractionated splenocytes population. **F,** transendothelial migration of D2A1 cells (fold increase compared to control RPMI medium) in the presence of conditioned medium from the Ly6G$^+$-enriched subpopulation of splenocytes from non-tumor-bearing or 4T1 mice. **G,** MMP8 and MMP9 secretion by an equal number of splenocytes from naïve BALB/c or 4T1-bearing mice. **H,** transendothelial migration (fold increase compared to control RPMI) of D2A1 cells in the presence of the indicated conditioned media, inhibitor or antibody against MMP8 or antibody against MMP9. At least 3 experiments were performed in duplicate. **I,** immunofluorescent staining of MMP9 (green) and Ly6G (red) in lungs of naïve BALB/c and 4T1 mice (implanted with 4T1 cells 4 weeks earlier). Scale bar, 25 μm. **J,** adoptive transfer of splenocytes from WT or MMP9 KO tumor-bearing mice (implanted with B16-F10-G-CSF–overexpressing cells 3 weeks earlier). Donor splenocytes were injected into WT or MMP9 KO recipient mice, as indicated. Experiment was terminated 2 weeks later, and pulmonary metastases of GFP-labelled B16-F10 cells were quantified. *, $P < 0.05$.

Published OnlineFirst April 12, 2016; DOI: 10.1158/2159-8290.CD-15-1157

within 2 hours of i.v. injection, a significantly higher proportion of the MDA-MB-231 tumor cells had extravasated from the luminal to the parenchymal side of endothelial walls in the 4T1 mice relative to their behavior in naïve mice. Hence, neutrophils mobilized by 4T1 cells accelerated the kinetics of extravasation of carcinoma cells that had previously lodged within pulmonary microvessels.

Neutrophils Facilitate Extravasation of Tumor Cells in an MMP-Dependent Manner

We undertook to study in more detail the mechanisms by which extravasation of intraluminal carcinoma cells was enhanced by the presence of splenocytes. Thus, we asked whether conditioned medium from splenocytes would enhance transendothelial migration in an *in vitro* model, in which transwell-permeable filter inserts were coated with either bEnd.3 murine endothelial cells or human umbilical vein endothelial cells (HUVEC). Conditioned medium from splenocytes of tumor-free mice slightly increased the transendothelial migration of D2A1 cells relative to unconditioned medium, whereas medium conditioned by splenocytes from 4T1 tumor–bearing mice led to a 3-fold increase in the ability of D2A1 cells to traverse the endothelial sheet of HUVECs (Fig. 4B and C). Similar results were obtained when the Transwell membranes were coated with bEnd.3 murine endothelial cells and when the migration of B16-F10 tumor cells was tested (Fig. 4D). These observations demonstrated that splenocytes from 4T1-bearing mice secrete soluble factors that enhance transendothelial migration of cancer cells.

The work described above had allowed us to associate most of the systemic effects of 4T1 cells with the mobilization specifically of neutrophils. Moreover, the percentage of $CD11b^+/Ly6G^+$ neutrophils within the splenocyte population was substantially elevated (21-fold) in 4T1 mice relative to naïve mice (Supplementary Fig. S4). Accordingly, we wished to confirm that neutrophils were responsible for facilitating transendothelial migration of cancer cells. To do so, we enriched for $Ly6G^+$ neutrophils from the spleens of 4T1 mice and collected conditioned medium from these cells as well as from unfractionated splenocytes containing an equal number of neutrophils. In fact, the medium conditioned by the $Ly6G^+$-enriched splenocytes from control mice increased transendothelial migration of D2A1 cells to a similar extent as the medium conditioned by unfractionated splenocytes prepared from 4T1 mice (Fig. 4E). Hence, $Ly6G^+$ neutrophils present in the spleens of 4T1 mice were indeed responsible for the lion's share of the observed enhanced transendothelial migration.

We undertook to determine whether neutrophils from 4T1-bearing mice were qualitatively different from normal neutrophils in their ability to promote transendothelial migration. To do so, we enriched splenocytes from non–tumor-bearing naïve mice for $Ly6G^+$ neutrophils. Conditioned medium from these cells increased transendothelial migration of D2A1 cells to the same extent as did medium conditioned by comparable numbers of $Ly6G^+$ cells prepared from 4T1 mice (Fig. 4F). Therefore, individual neutrophils from tumor-bearing and non–tumor-bearing mice were equally competent to facilitate extravasation, and the cell-biologic effects of splenocytes from tumor-bearing mice, including the enhanced transendothelial migration described above (Fig. 4D), reflected an expansion in the numbers of neutrophils and therefore a corresponding amplification of their normal intrinsic biologic properties.

We undertook to identify the soluble factors secreted by neutrophils that enhanced the transendothelial migration of the tumor cells. Using antibody arrays, we found higher levels of secretion of two proteases, MMP8 and MMP9, in splenocytes from 4T1 mice relative to the medium conditioned from the same number of splenocytes extracted from naïve mice. These findings were further verified by ELISA (Fig. 4G). Inhibition of MMP8 with either a specific small-molecule inhibitor or a neutralizing antibody reduced the rate of transendothelial migration to basal levels observed in unconditioned medium (Fig. 4H). An anti-MMP9 antibody also reduced by more than 50% the ability of splenocyte-conditioned medium to enhance transendothelial migration (Fig. 4H). Overall, these results indicated that splenocyte-secreted MMP8 and MMP9 played an important role in mediating the *in vitro* transendothelial cell migration of tumor cells. Importantly, high levels of MMP8 and MMP9 were secreted into the medium by $Ly6G^+$ neutrophils (data not shown), further emphasizing the key role of neutrophils in promoting metastasis by aiding tumor cell extravasation.

As reported by others (11, 12, 33), we noted the abundant expression of MMP9 in the lungs of 4T1 tumor–bearing mice but not in those of control mice. Furthermore, MMP9 is expressed by $Ly6G^+$ neutrophils (Fig. 4I). We used MMP9 knockout (KO) mice (46) to further dissect the contribution of this particular protease to metastasis using isogenic B16-F10–G-CSF rather than 4T1 cells to mobilize neutrophils in the C57BL/6 genetic background. Equal numbers of the splenocytes from these tumor-bearing wild-type (WT) and MMP9 KO host mice were then injected into recipient mice followed by i.v. injection of B16-F10-GFP^+ cells (1 hour later). As expected, the adoptive transfer of WT splenocytes into WT recipient mice resulted in a 5-fold increase in metastasis relative to control mice that did not receive splenocytes. In contrast, no significant increase was observed following adoptive transfer of MMP9 KO splenocytes into MMP9 KO recipient mice. Importantly, when MMP9 WT splenocytes were transferred into MMP9 KO recipient mice, a 5-fold increase in B16-F10 lung metastases was noted, similar to the effect achieved by adoptive transfer of WT splenocytes into WT recipient mice (Fig. 4J). This indicated that the splenocyte-derived protease MMP9 played a major role in facilitating transendothelial migration both *in vitro* and, more importantly, *in vivo*, the latter process contributing to enhanced formation of metastases. These data collectively argue that, in addition to their role in suppressing NK cell–mediated clearance of tumor cells, neutrophils promote metastasis by enhancing the extravasation of these cells.

Neutrophil-Secreted IL1β Activates Endothelial Cells and Facilitates Migration

The enhanced extravasation clearly involved an interplay between three cell types: the extravasating tumor cells, the neutrophils, and the endothelial cells. To further dissect the components of this cross-talk, we first looked for a direct effect of the neutrophils on either the tumor cells or the endothelial

Published OnlineFirst April 12, 2016; DOI: 10.1158/2159-8290.CD-15-1157

cells individually. To test this, we conducted experiments in which only the D2A1 tumor cells or the endothelial cells were pretreated with the 4T1 splenocyte–conditioned medium for 3 hours. The pretreated cells were washed to remove any residue of the conditioned medium prior to the addition of these D2A1 cells to the top chamber of Transwells in which the membranes had been coated with endothelial cells. This protocol contrasts with that used in the experiments depicted in Fig. 4B, in which the migration occurred in the presence of conditioned medium. As indicated in Fig. 5A, pretreatment of the D2A1 cells alone did not increase their ability to migrate through the endothelial cell layer. In stark contrast, pretreatment of murine endothelial bEnd.3 cells with the 4T1 splenocyte–conditioned medium indeed sufficed to increase transendothelial migration of D2A1 cells (Fig. 5B). Furthermore, incubation of bEnd.3 cells with 4T1 splenocyte–conditioned medium induced expression and secretion of MMP9 by the endothelial cells, augmenting that initially produced by the neutrophils (Fig. 5C, and Supplementary Fig. S5A and S5B). These results suggest that the enhanced extravasation does not result from a direct effect of the neutrophils on the migrating tumor cells but instead through the modulation of the endothelial cell barrier.

Immune cells affect their surroundings through the secretion of cytokines and chemokines. More specifically, IL1β is a cytokine that is known to be secreted by neutrophils, to activate endothelial cells, and to increase leukocyte extravasation (16). We therefore tested whether IL1β plays a role in the activation of the endothelial cells in our system, and, indeed, a 2-fold increase in transendothelial migration of D2A1 cells was observed when IL1β was added to RPMI medium (Supplementary Fig. S5C). Furthermore, ~4-fold higher levels of IL1β were secreted into the conditioned medium by splenocytes from 4T1 mice compared to splenocytes from control BALB/c mice (Fig. 5D). Importantly, the levels of IL1β secreted by Ly6G$^+$ neutrophils (enriched from spleens of 4T1 mice) were similar to those secreted by the 4T1 splenocyte population, pointing once again to the important role neutrophils play in IL1β-mediated responses. Moreover, transendothelial migration *in vitro* was reduced when an IL1 receptor antagonist was added to conditioned medium from splenocytes obtained from 4T1 mice (Fig. 5E). Furthermore, upon the addition of an IL1 receptor antagonist to the conditioned medium, MMP9 secretion by endothelial cells following treatment with 4T1 splenocyte-conditioned medium was inhibited (Fig. 5F). Taken together, these observations indicated that neutrophil-secreted IL1β acts directly to activate the endothelial cells, ostensibly amplifying the effects of the already-high levels of MMP9 found in the 4T1 splenocyte–conditioned medium.

Activated Endothelial Cells Enable Expedited Protrusion Formation by Intraluminal Tumor Cells

To further decipher precisely how activated endothelial cells enable enhanced transendothelial migration, we used an *in vitro* assay featuring perfusable microvasculature formed in microdevices (47). In this model, HUVECs are suspended in a fibrin/collagen type I matrix and interconnected vascular networks are formed via a vasculogenic-like process over a period of 4 to 5 days in microdevices. In this assay, tumor cells can be infused and are found to arrest via physical trapping, mimicking the *in vivo* process. Extravasation rate was quantified via confocal microscopy at 20× and scored as the subset of cells that had completely traversed the endothelial barrier (Fig. 6A).

HUVEC networks were treated with 4T1 splenocyte–conditioned medium (or control RPMI) for 4 hours prior to the addition of human MDA-MB-231 cells to the devices. We found that 16.2% of MDA-MB-231 human breast cancer cells extravasated from the microvessels formed by control HUVECs within 3 hours. This extravasation efficiency was increased ~2.5-fold when HUVECs were pretreated with 4T1 splenocyte–conditioned medium (Fig. 6A and B).

In order to study and understand the transendothelial migration of the tumor cells in further detail, we tracked the transendothelial migration of MDA-MB-231 cells using time-lapse confocal microscopy. We first noted that the initial sign of transendothelial crossing of tumor cells appeared as small protrusions extending from the cell bodies of these carcinoma cells through the endothelial layer.

Analysis of image sequences of transmigrating MDA-MB-231 revealed that the time required for tumor cells to extend the first initial, discernible protrusion through the endothelial wall was significantly shorter when HUVECs were pretreated with 4T1 splenocyte–conditioned medium (compared to RPMI medium control). Thus, following pretreatment of HUVECs with 4T1 splenocyte–conditioned medium, ~5% of MDA-MB-231 had already extended protrusions after 15 minutes following tumor perfusion, whereas the same degree of protrusion formation occurred in control-treated devices only after 1 hour (Fig. 6B). The average time for the first observed protrusion was ~30 minutes for 4T1-conditioned medium-treated HUVECs, compared to ~90 minutes for the control RPMI (Fig. 6C). However, the time required for MDA-MB-231 cells to migrate across the endothelial cell layer—i.e., the amount of time required for a cell from the first observable protrusion until complete translocation across the endothelial barrier—was not different between treated versus untreated HUVECs (~50 minutes; Fig. 6D).

These results further strengthen the findings reported above, demonstrating that the neutrophils facilitate the migration of tumor cells in an indirect manner—not through a direct effect on the tumor cells but rather through their activation of endothelial cells, which in turn expedite the initiation of transendothelial crossing by tumor cells.

DISCUSSION

As the biologic complexity of tumor growth and metastasis is explored in greater detail, it has become apparent that key aspects of tumor biology can be explained only by a detailed understanding of how various types of host cells contribute to tumor progression. The work presented here describes how recruited host cells can affect the behavior of cancer cells that have traveled from primary tumors to a distant anatomical site, specifically the lungs. Such effects, by necessity, reflect changes in the systemic physiology of tumor-bearing hosts and govern later steps of the invasion–metastasis cascade. More specifically, we find that Ly6G$^+$ neutrophils can increase

Published OnlineFirst April 12, 2016; DOI: 10.1158/2159-8290.CD-15-1157

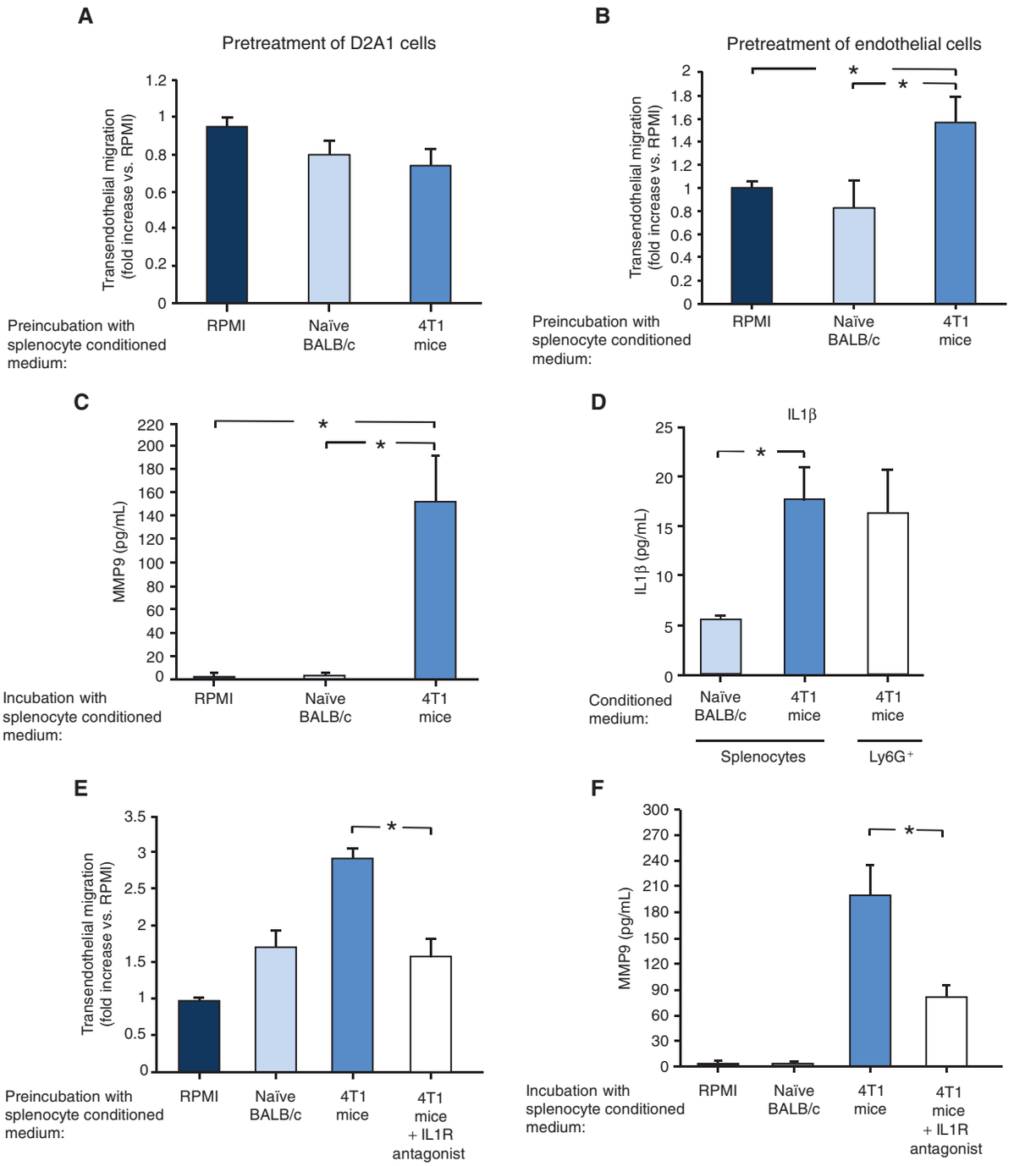

Figure 5. Neutrophil-secreted IL1β activates endothelial cells and facilitates migration. **A,** transendothelial migration (fold increase compared to control RPMI medium) of D2A1 cells following pretreatment of bEnd.3 cells with the indicated conditioned media (prepared from equal numbers of splenocytes). The inserts were washed with RPMI medium prior to the addition of the D2A1 cells. Five experiments were performed in duplicate. **B,** transendothelial migration (fold increase compared to control RPMI medium) of D2A1 cells following pretreatment of bEnd.3 cells with the indicated conditioned media (prepared from equal numbers of splenocytes). The inserts were washed with RPMI medium prior to addition of the D2A1 cells. Five experiments were performed in duplicate. **C,** secretion of MMP9 by bEnd.3 cells following incubation of the endothelial cells with 4T1 splenocyte–conditioned medium or splenocyte-conditioned medium from control non–tumor-bearing mice (prepared from equal numbers of splenocytes) as determined by ELISA. **D,** secretion of IL1β by splenocytes from naïve BALB/c mice, splenocytes from 4T1 mice, or Ly6G$^+$ neutrophils enriched from splenocytes from 4T1 mice. Levels of IL1β secreted into the conditioned medium were determined by ELISA of at least 5 samples per group. **E,** transendothelial migration (fold increase compared to control RPMI) of D2A1 cells following preincubation of bEnd.3 cells with the indicated conditioned media and in the presence of IL1 β receptor antagonist. At least 4 experiments were performed in duplicate. **F,** secretion of MMP9 by bEnd.3 endothelial cells following incubation of the endothelial cells with splenocyte-conditioned medium from control non–tumor-bearing mice, 4T1 tumor–bearing mice or 4T1 tumor–bearing mice together with IL1 receptor antagonist. MMP9 secretion was determined by ELISA of at least 5 samples per treatment. *, $P < 0.05$.

Published OnlineFirst April 12, 2016; DOI: 10.1158/2159-8290.CD-15-1157

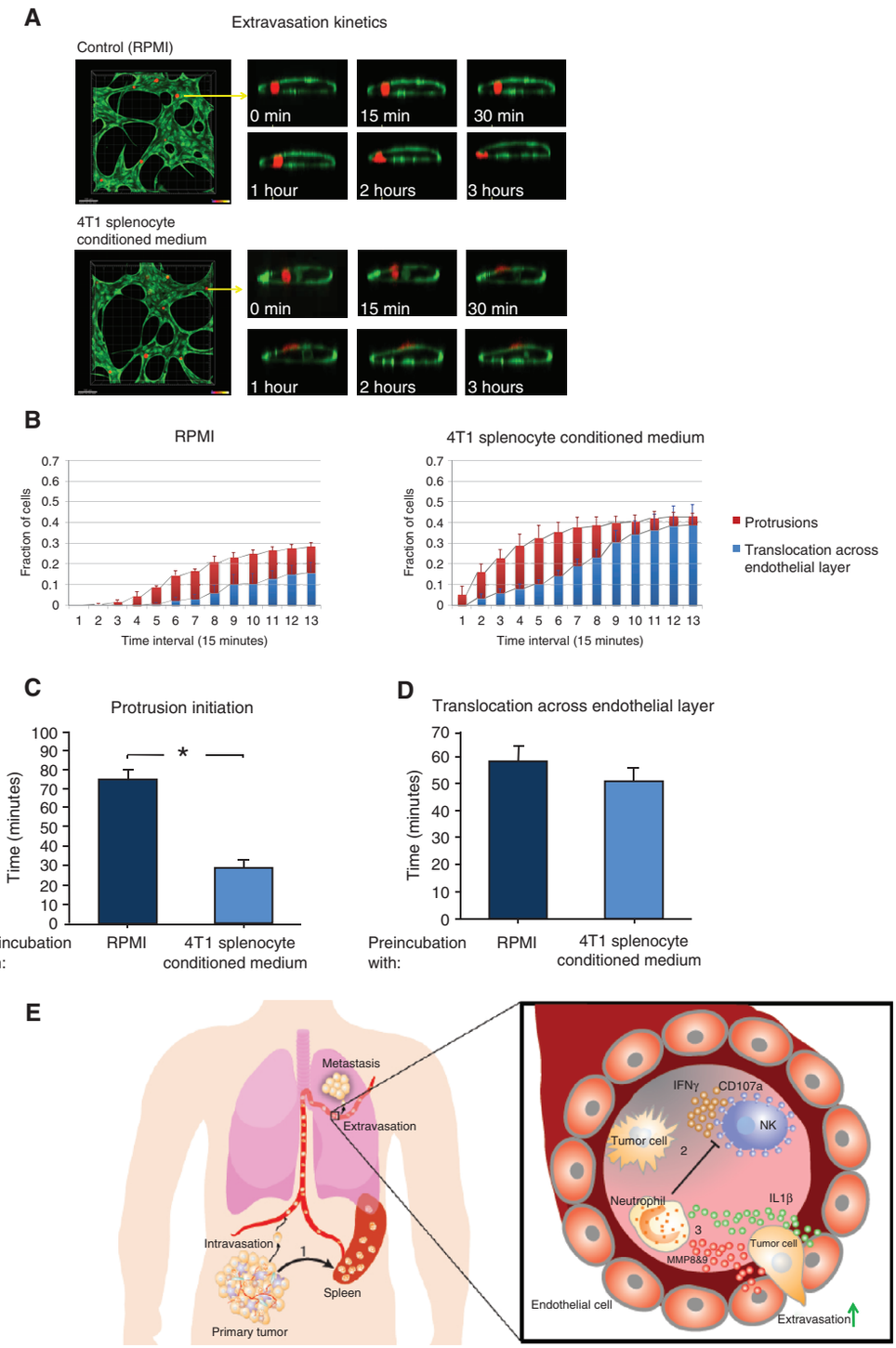

Figure 6. Visualization of protrusion and extravasation dynamics of tumor cells. **A,** left, high-resolution time-lapse confocal microscopy (20×) of an extravasating MDA-MB-231 cell (red) immediately after seeding in microvasculature network (HUVECs labeled in green). Right, confocal images taken at a single slice tracking a tumor cell as it transmigrates through the endothelium and into the 3-D matrix over a period of 3 hours. Scale bars, 100 μm. **B,** protrusion formation (red) and extravasation (blue) rates of MDA-MB-231 cells in HUVEC vessels that had been pretreated with 4T1 splenocyte–conditioned medium or control (RPMI). **C,** time required for protrusion formation (i.e., partial translocation across the lumen) and **D,** time required for complete extravasation (i.e., the entire cell body has cleared the lumen) of MDA-MB-231 cells in HUVEC vessels that had been pretreated with 4T1 splenocyte conditioned medium or control (RPMI). Data were collected from >150 cells per condition, over 3 independent experiments. **E,** events leading to metastasis of circulating tumor cells: (1) primary tumor perturbs distant organs, leading to neutrophil expansion and mobilization. (2) Neutrophils increase intraluminal survival of circulating tumor cells by inhibiting their clearance by NK cells. (3) Neutrophils increase extravasation of circulating tumor cells through secretion of IL1β and MMPs. *, $P < 0.05$.

Published OnlineFirst April 12, 2016; DOI: 10.1158/2159-8290.CD-15-1157

metastatic seeding in at least two distinct ways: (i) by inhibiting NK-cell cytotoxic activity, the neutrophils can protect intraluminally trapped tumor cells from rapid clearance by these innate immune cells, and (ii) by expediting extravasation. Both of these mechanisms contribute to the ultimate formation of metastases by increasing the pool of tumor cells that succeed in entering the lung parenchyma, placing them in sites where they are poised to generate micrometastases and, subsequently, macroscopic metastases (Fig. 6E).

Previous reports have suggested that tumors are able to modify the distant microenvironment prior to the arrival of metastatic cells, doing so by creating a "premetastatic niche" (48–50). In this "premetastatic niche" model, bone marrow–derived cells were reported to arrive in the lung parenchyma days before tumor cells and create a more hospitable environment that facilitates colonization and subsequent formation of macroscopic metastases. We demonstrate here a quite different mechanism, in which the accessory effects of neutrophils operate only in a relatively short window of time during which neutrophils suppress the otherwise-rapid NK cell–mediated clearance of intraluminally trapped carcinoma cells and facilitate the extravasation of these cells through effects on endothelial cells.

Our observations demonstrate a clear prometastatic role for the Ly6G$^+$ neutrophils and are supported by other reports showing that Gr1$^+$-CD11b$^+$ cells alter the overall landscape of the metastatic lung and tip the balance of immune protection in favor of tumor promotion (12, 33). Others have shown an antimetastatic effect for neutrophils in 4T1 tumor–bearing mice (11). These antimetastatic properties were demonstrated in neutrophils that accumulate in the lung prior to metastasis formation (i.e., up to day 10 after initial 4T1 tumor implantation), whereas our own work examines these dynamics in a later phase when implanted tumor cells have already formed significant primary tumors and have proceeded to seed and colonize distant tissues (14–31 days after 4T1 tumor implantation). The role of neutrophils in metastasis may be context dependent, and it is plausible that the early tumor-entrained neutrophils and their later counterparts exert opposite functions on metastatic progression in the lungs. Further studies may shed light on the role of neutrophils in the formation of various types of metastases.

Although our present results demonstrate that Ly6G$^+$ neutrophils directly promote pulmonary metastasis of cancer cells through at least two distinct mechanisms, it remains possible that other types of innate immune cells promote metastasis in other cancers and anatomical sites by acting through alternative mechanisms. For example, recent studies have reported a role for the cytokine CCL2 in promoting metastasis in models of breast and colon carcinoma through recruitment of monocytes to the lung (51, 52) as well as by activating endothelial cells, doing so by signaling through their CCR2 receptors (53). Platelets have also been shown to play a role in facilitating metastasis through the secretion of CXCL5 and CXCL7, which recruit granulocytes to sites of intraluminally trapped tumor cells (54). Altogether, these results point to the complexity of the intraluminal survival and extravasation steps, in which different types of immune cells, cytokines, and proteases appear to participate.

Tumor cells have been shown to recruit immune-suppressive cells that erect a protective barrier against immune attack (55–58). These suppressive actions have been studied mostly in the context of the monocyte/macrophage subset of CD11b$^+$/Gr1$^+$ myeloid cells and their role in suppression of T-cell–mediated responses (59, 60). The fact that we observed comparable effects in immune-competent mice as well as immune-deficient NOD/SCID mice indicates that the mechanism of action in our model system utilizes a different type of immune suppression. Furthermore, our data highlight an immunosuppressive role that is unique in two aspects: (i) the immune cells involved—neutrophils—act through their inhibition of NK cell–mediated clearance of cancer cells; and (ii) the time frame of the immunosuppression—during a short window of time beginning with the arrival of disseminated cancer cells in the microvessels of a target organ, in this case the lung.

The present results show that the neutrophils activate and induce changes in endothelial cells, leading to increased extravasation through the action of MMP9. An additional mechanism for this direct activation of endothelial cells might well be mediated through vascular endothelial growth factor (VEGF). Although several proteinases are capable of releasing VEGF from the ECM, MMP9 is especially efficient in this regard (61, 62). Along these lines, the increase in MMP9 levels that we observed in splenocyte-conditioned medium from 4T1 mice was accompanied by a concomitant increase in the levels of VEGF (compared to splenocyte-conditioned medium from control naïve mice; data not shown). This cross-talk between neutrophils and endothelial cells and the specific roles of MMP9 and VEGF in facilitating extravasation warrant further research.

4T1-induced tumors represent a widely used model system in mice used to study metastasis. The effects of the neutrophilia that we observed in tumor-bearing mice are consistent with clinical data showing that either elevated neutrophil counts or elevated neutrophil/lymphocyte ratios serve as indicators of poor prognoses in a variety of cancers, including lung, pancreatic, ovarian, gastric, and colon carcinomas (63–67). Furthermore, elevated plasma G-CSF levels have been reported in a variety of solid tumors and found to be associated with severe leukocytosis and poor prognosis (68–72).

In oncologic practice, G-CSF is often used to overcome chemotherapy-associated neutropenia (73). Importantly, the present findings and those of others (12, 14) suggest that such G-CSF may, in certain circumstances, actually serve to facilitate tumor metastasis. In particular, our data indicate that G-CSF administration has prometastatic effects not only in the case of prolonged exposure to high levels of G-CSF secreted by the primary tumor but even following short-term (5 days) systemic administration of this cytokine. Other reports have shown in experimental mouse models that overexpression of G-CSF by tumors has a deleterious impact on therapeutic outcome, because it mediates tumor refractoriness to anti-VEGF therapy (14). Although it may be necessary to administer G-CSF to overcome the acute neutropenia of certain patients, identifying and eliminating specific tumor-promoting activities induced by G-CSF may eventually yield more beneficial clinical outcomes for patients with cancer who are suffering neutropenia.

Published OnlineFirst April 12, 2016; DOI: 10.1158/2159-8290.CD-15-1157

METHODS

Cell Culture

All cells were cultured in a 5% CO_2 humidified incubator at 37°C. Mouse mammary carcinoma cell lines 4T1 (ATCC) and D2A1 (gift from F.R. Miller, Wayne State University, Detroit, MI) were grown in RPMI supplemented with 10% heat inactivated FBS, 100 U/mL penicillin, and 100 μg/mL streptomycin (Invitrogen). Murine endothelial, B.end3 cells were grown in DMEM, supplemented with 10% FBS, 100 U/mL penicillin, and 100 μg/mL streptomycin. HUVECs were propagated in endothelial cell basal medium (EBM) with 0.1% human epidermal growth factor (hEGF), 0.1% hydrocortisone, 2% FBS, 0.4% bovine brain extract (BBE), 30 μg/mL gentamicin, and 15 ng/mL amphotericin. MDA-MB-231 cells were grown in DMEM/F12 supplemented with 10% FBS, 100 U/mL penicillin, and 100 μg/mL streptomycin. B16-F10 cells were grown in DMEM supplemented with 10% heat-inactivated FBS, 100 U/mL penicillin, and 100 μg/mL streptomycin (Invitrogen). YAC-1 cells were grown in RPMI supplemented with 10% FBS, 100 U/mL penicillin, and 100 μg/mL streptomycin (Invitrogen). In experiments testing *in vitro* extravasation in microvasculature networks, HUVECs stably expressing GFP (Angioprotemie) were cultured in EGM-2MV medium (Lonza) and used at passages 4 to 6. Normal human lung fibroblasts (Lonza) were cultured in complete fibroblast growth medium (Lonza) and used between passages 4 to 8. Cells that were stably infected with GFP or tdTomato were done so as previously described (36). In order to overexpress G-CSF, lentiviral vectors expressing the G-CSF protein coding DNA (MMM1013-99829324; Open Biosystems) were generated using the pLV-IRES-neo as a backbone. D2A1 and B16-F10 cells were then infected with the lentiviral vectors. Cell lines were not authenticated prior to use.

Animals

All research involving animals complied with protocols approved by the MIT Committee on Animal Care. BALB/c mice, C57BL/6 mice, and CB6F1 mice (a cross between BALB/c and C57BL/6) were obtained from The Jackson Laboratory. A colony of NOD-SCID mice was maintained in-house. The MMP9 KO mice (Stock # 007084) were originally obtained from The Jackson Laboratory.

Tumor Models

For primary tumor formation, 2.5×10^5 4T1, D2A1, or B16-F10 tumor cells were injected s.c. in their growth medium with 20% Matrigel into 10-to-14-week-old female syngeneic BALB/c or C57BL/6 (for B16-F10 cells) mice. For contralateral injections, 2.5×10^5 4T1 tumor cells were injected s.c. on the right, and at the same time, 2.5×10^5 D2A1-Tom$^+$ tumor cells were injected s.c. on the left side of the same mouse. For i.v. injections, 2×10^4 cells were injected in 100-μL volume into mice. Splenectomy was performed as previously described (34). Five hours after splenectomy, tumor cells were injected s.c. The contralateral experiments and the splenectomy experiments were terminated 4 to 5 weeks after tumor cell implantation, at which time leukocyte mobilization as well as pulmonary metastasis was scored. In experiments assessing lung macrometastasis formation following i.v. injection, D2A1, B16-F10, and MDA-MB-231 cells (2×10^4) were injected i.v. into BALB/c mice (for D2A1 cells) or NOD/SCID mice (for B16-F10 and MDA-MB-231 cells) implanted with 4T1 cells 2 weeks earlier (or control non–tumor-bearing mice), experiments were terminated, and metastasis was scored 14 days later. In experiments testing short-term retention of tumor cells (NK-cell clearance and extravasation; 2–24 hours after i.v. injection), the cells were injected into mice implanted with 4T1 cells 4 weeks earlier (or control non–tumor-bearing mice). In compliance with veterinary guidelines, experiments in which C57BL/6 mice were implanted with B16-F10-G-CSF cells (or B16-F10 cells overexpressing control vector) were terminated 3 weeks after tumor cell implantation.

Splenocyte and Neutrophil Adoptive Transfer

In experiments involving adoptive transfer of splencoytes or Ly6G$^+$ neutrophils, spleens were removed from donor mice and homogenized into a single-cell suspension using a 3-mL syringe plunger and 40-μm cell strainer (BD Falcon). Thereafter, splenocytes were passed through a 40-μm filter basket prior to injection. In experiments involving adoptive transfer of neutrophils, splenocytes were enriched for Ly6G$^+$ neutrophils using the MACS cell separation kit (Miltenyi Biotec) according to the manufacturer's instructions. Mice were injected i.v. with 2 injections of splenocytes (2.5×10^7–3×10^7) or Ly6G$^+$ neutrophils (5×10^6–6×10^6) suspended in 200 μL medium per injection, 45 minutes apart (control mice were injected with vehicle). D2A1-Tom$^+$ cells or B16-F10-GFP$^+$ cells (2×10^4 cells in 100 μL medium) were injected i.v. 45 minutes after the last splenocyte or neutrophil injection.

Quantification of Lung Metastases

For visualizing cancer cells that had disseminated in the lung tissue, lungs were harvested from the injected mice, dissected into the five lobes, and analyzed under a fluorescence dissection microscope (Leica MZ12) for the presence of tdTomato$^+$- or GFP$^+$-labeled microscopic and/or macroscopic lung metastases. The quantification of cells retained in the lungs 10 minutes, 1 hour, 2 hours, 4 hours, or 24 hours after i.v. injection was performed by directly counting the numbers of GFP$^+$ cells or tdTomato$^+$ cells in the lung under a fluorescence dissection microscope (Leica MZ12). For the quantification of lung metastases in mice carrying unlabeled 4T1 tumors, lungs were fixed in 10% formalin, embedded in paraffin, sectioned and stained with hematoxylin and eosin. YAC-1 cells were labeled with Cell Trace CFSE (Life Technologies) prior to i.v. injections (2×10^4 cells) according to the manufacturer's instructions.

In Vivo *Imaging*

Bioluminescence imaging of luciferase activity was used to monitor cancer cell clearance with a Xenogen IVIS system under 2.5% isoflurane anesthesia at the indicated time points as described. Imaging of mice was performed by injection of d-luciferin (165 mg/kg of body weight, i.p. injection; Caliper Life Sciences), 10 minutes before bioluminescence imaging. Images were analyzed using Living Image Software version 4.3.1 (Caliper Life Sciences).

NK Cell and Neutrophil Depletion

To deplete NK cells, anti-asialo GM-1 (20 μL per mouse, clone Poly21460; BioLegend) or anti-NK1.1 (cat #BE0036; Bioxcell) antibodies were injected i.p. 1 day prior to tumor cell injections. Matching isotype Rabbit polyclonal IgG (AB-105-C; R&D Biosystems) served as a control. To deplete neutrophils, anti-Ly6G antibody (200 μg per mouse, clone 1A8; BioXCell) was injected i.p. 1 day prior to tumor cell injections. Matching isotype Rat IgG2A (MAB006; R&D Biosystems) served as a control.

In Vivo *Extravasation*

In vivo extravasation assay was performed as previously described (74). FITC-conjugated anti-human HLA-2 antibody (20 μg/mouse in 100 ul volume of PBS, clone BB7.2; BD Biosciences) was injected i.v. into NOD/SCID mice 2 hours after i.v. injection of 1×10^5 MDA-MB-231-Tom$^+$ cells. Lungs were harvested 10 minutes after injection of antibody, digested with collagenase A (1.5 mg/mL), hyaluronidase (125 u/mL), and DNAse (0.1 mg/mL) for 1 hour at 37°C. Resulting cell suspensions were filtered through 70-μm pore-size nylon meshes. Cells were incubated in the presence of saturating amounts (10 μg/sample) of unlabeled anti–HLA-A2 Ab for 30 minutes. The percentage of MDA-MB-231-Tom$^+$ cells that were labeled with FITC-HLA-A2 antibodies was determined by flow cytometry.

Published OnlineFirst April 12, 2016; DOI: 10.1158/2159-8290.CD-15-1157

In Vivo *G-CSF Administration*

To assess the effects of G-CSF on metastasis, BALB/c mice were injected s.c. with rhG-CSF (250 mg/kg; Neupogen, Amgen) daily for 5 consecutive days. Control animals were given PBS as a vehicle. Five hours after the last G-CSF injection, 2×10^4 D2A1 cells were injected i.v. In other experiments, the effect of adoptive transfer of splenocytes from G-CSF–treated mice was tested. Five hours after the last G-CSF injection, spleens were harvested from G-CSF–treated mice (or control PBS-treated mice) and adoptive transfer into recipient BALB/c mice followed by i.v. injection of D2A1 cells was done as previously described in the Splenocyte and Neutrophil Adoptive Transfer section.

Preparation of Splenocyte-Conditioned Media

Splenocyte-conditioned media were prepared either from 1.5×10^7 freshly isolated unsorted splenocytes or from the Ly6G$^+$ enriched subpopulation. These freshly isolated cells were plated in the presence of 10 mL RPMI medium (supplemented with 10% heat-inactivated FBS, 100 U/mL penicillin, and 100 μg/mL streptomycin) for 48 hours at 37°C, 5% CO_2 in a humidified incubator. Subsequently, the conditioned medium was collected, and the cells were removed by centrifugation. The supernatant was collected and sterile filtered through a 0.2-μm Acrodisc filter (PALL Biosciences).

ELISA and Protein Arrays

Plasmas and conditioned media were analyzed for mouse G-CSF (MCS00; R&D Systems), IL1β (MLB00B; R&D Systems), MMP9 (MMP900B; R&D Systems), and MMP8 (USCN Life Science Inc.) according to the manufacturer's instructions. Conditioned media from splenocytes or tumor cell lines were analyzed for the secretion of various proteins using mouse angiogenesis array (ARY015; R&D Systems) and mouse cytokine array (ARY006; R&D Systems) according to the manufacturer's instructions.

In Vitro *Transendothelial Migration Assay*

The upper surface of 8-μm polyester Transwells (PET; corning) was coated with 5×10^4 mouse endothelial cells for 24 hours at 37°C in complete bEnd.3 mEC media (100 μL in the upper chamber and 500 μL in the lower well). Once the endothelial cell layer had been established, tumor cells (5×10^4) were added to the upper chamber. The lower compartments of the wells were filled with RPMI medium (supplemented with 10% FBS) or splenocyte-conditioned media (prepared as described above). In the inhibition experiments, 5 ng/mL IL1β receptor antagonist (Prospec), 1 μg of anti-MMP9 antibody (ab38898; Abcam) or anti-MMP8 antibody (ab53017; Abcam) was added to the upper chamber. MMP8 inhibition on the transendothelial migration of D2A1 tumor cells was also tested using 10, 50, or 100 μmol/L of MMP8 inhibitor-1 (Calbiochem); wells supplemented with RPMI containing 0.1% DMSO were included in the analysis as controls. For the preconditioning experiments, D2A1-Tom$^+$ cells or mouse endothelial cells were treated with conditioned medium from splenocytes obtained from naïve BALB/c or 4T1 mice, or RPMI (control) for 4 hours. The pretreated endothelial cells or D2A1-Tom$^+$ cells were washed in PBS to remove any residue of the conditioned medium prior to the addition of D2A1 cells to the top chamber of Transwells. Migration was assessed after 4 hours at 37°C in 5% CO_2. The cells from the upper surface of the well were wiped off with PBS, and the number of migrated cells were counted in 4 fields. Experiments were repeated at least 5 times and performed in duplicate or triplicate.

Microvascular Network Extravasation Assay

Perfusable *in vitro* microvascular networks were generated in microfluidic devices as described previously (47). Briefly, HUVECs and normal human lung fibroblasts were resuspended in fibrin gels at 6×10^6 cells/mL and 3×10^6 cells/mL, respectively, and injected into micro channels. Devices were then cultured in EGM-2MV for 4 days at 37°C in 5% CO_2, after which lumens formed and became perfusable. Four hours prior to tumor cell injection, media in devices were changed to splenocyte-conditioned media or control RPMI. Then, MDA-MB-231 Td Tomato were resuspended to 5×10^5 cells/mL in either conditioned media or RPMI (Company) and perfused into corresponding devices via a hydrostatic pressure drop. Devices were transferred to an environmental chamber equipped with confocal microscopy (Olympus FV1000). Time-lapse images were taken every 15 minutes for at least 4 hours at 20× magnification and z-steps of 1.7 μm. Images were analyzed using Imaris Bitplane software. A cell is defined as extravasated when the entire cell body has cleared the lumen, based on the orthogonal views given in Imaris. As soon as a cell becomes partially translocated past the lumen, it is defined as "protrusive." The same individual cells were followed over a period of 4 hours. Data were collected from >150 cells per condition, over 3 independent experiments.

WBC Counts in Peripheral Blood

To obtain peripheral WBC counts, mice were bled retro-orbitally. For WBC counts, an aliquot was diluted 1:10 in 1× PBS and processed at the MIT Division of Comparative Medicine.

Flow Cytometry

Cells were labeled for flow cytometry by incubation with the following fluorophore-conjugated antibodies: CD3 perCP-Cy5.5 (17A2; BioLegend), Cd49b PE (DX5; BioLegend), NKp46 APC (29A1.4; BioLegend), CD11b FITC (M1/70; eBioscience), Ly6G PE (1A8; BD Pharmingen), G-CSF Receptor (S1390; Abcam), CD107a (1D4B; BioLegend). Flow cytometric analyses were carried out on a FACS Fortessa (BD Biosciences) using BD FACSDiva Software.

Ly6G$^+$ Neutrophil Enrichment

Spleens of tumor-bearing and control mice were homogenized with the GentleMACS (Miltenyi Biotech), according to the manufacturer's instructions in order to obtain a single-cell suspension. Splenocytes were counted, and 1×10^8 to 2×10^8 cells were enriched for Ly6G$^+$ cells using magnetic beads (130-092-332, Miltenyi Biotech) according to the manufacturer's instructions. The purity of the Ly6G$^+$ population was assessed by FACS analysis.

Ex Vivo *Degranulation Assay*

Wells of flat-bottomed, high-protein binding plates (Thermo Fisher Scientific) were coated with 0.5 μg of anti-NKG2D antibody (MI-6) or with 0.5 μg of anti-NKp46 antibody (29A1.4) or rat IgG2a as a control. A total of 10^6 cells per well were stimulated for 5 hours in the presence of 1 μg of Golgi Plug (BD), 1 μg of Golgi Stop (BD), 100 U of recombinant human IL2 (Roche), and anti-CD107a (1D4B) mAb antibody.

Immunofluorescence

Serial frozen sections (6 μm) were prepared, and immunofluorescence staining was carried out for histologic analysis. After blocking the sections with 4% normal goat serum in PBS at room temperature for 30 minutes, MMP9 antibody (ab38898; Abcam) was incubated at 4°C overnight followed by Alexa Fluor 594 goat anti-rabbit IgG or Alexa Fluor 647 anti-rabbit IgG antibody (A11037 and A21245; Life Technologies). For double immunofluorescence staining, anti-Ly6G antibody (clone: 1A8, BioLegend) was incubated at room temperature for 1 hour followed by Alexa Fluor 488 goat anti-rat IgG (H+L) antibody (A11006; Life Technologies). Nuclei were stained with DAPI using VECTASHIELD Mounting Medium (H-1200; Vector Laboratories, Inc.) and images were captured using BX63 (Olympus) equipped with ANDOR Neo sCMOS Monochrome Camera (Andor Technology Ltd.). The images were processed using ImageJ software.

Published OnlineFirst April 12, 2016; DOI: 10.1158/2159-8290.CD-15-1157

Statistical Analysis

All of the data are presented as the mean ± SEM. An unpaired two-tailed Student *t* test was used to calculate the *P* values. A *P* value of less than 0.05 was considered statistically significant.

Disclosure of Potential Conflicts of Interest

R.D. Kamm has ownership interest (including patents) in AIM Biotech. No potential conflicts of interest were disclosed by the other authors.

Authors' Contributions

Conception and design: A. Spiegel, M.J. Pittet, R.A. Weinberg
Development of methodology: A. Spiegel, M.W. Brooks, M.B. Chen
Acquisition of data (provided animals, acquired and managed patients, provided facilities, etc.): A. Spiegel, M.W. Brooks, S. Houshyar, F. Reinhardt, M. Ardolino, E. Fessler, M.B. Chen, A. Iannello, Y. Iwamoto
Analysis and interpretation of data (e.g., statistical analysis, biostatistics, computational analysis): A. Spiegel, M.W. Brooks, S. Houshyar, M. Ardolino, E. Fessler, J. DeCock, A. Iannello, V. Cortez-Retamozo, M.J. Pittet, D.H. Raulet
Writing, review, and/or revision of the manuscript: A. Spiegel, M.W. Brooks, S. Houshyar, E. Fessler, J.A. Krall, J. DeCock, I.K. Zervantonakis, V. Cortez-Retamozo, R.D. Kamm, M.J. Pittet, D.H. Raulet, R.A. Weinberg
Administrative, technical, or material support (i.e., reporting or organizing data, constructing databases): S. Houshyar, M. Ardolino, I.K. Zervantonakis
Study supervision: A. Spiegel, R.D. Kamm, R.A. Weinberg

Acknowledgments

The authors thank R. Goldsby, T. Lapidot, S. Ben-Sasson, and R. Gazit for critical review of this manuscript and insightful discussions; Mahak Singhal and Paul Hager for technical assistance; Fred Miller for cells; Tsukasa Shibue for cells and materials; and members of the Weinberg laboratory for helpful discussions and materials. The authors thank the Core Flow Cytometry Facilities at Whitehead Institute for Biomedical Research, MIT Koch Institute Histology Facility for tissue sectioning, MIT Division of Comparative Medicine for analysis of blood differentials, and Tom DiCesare for graphical assistance. R.A. Weinberg is an American Cancer Society research professor and a Daniel K. Ludwig Foundation cancer research professor.

Grant Support

A. Spiegel was supported by fellowships from the Human Frontier Science Program (LT00728/2008-L), the Charles King Trust Foundation, and the Ludwig Fund for Cancer Research. M. Ardolino was supported by a Cancer Research Institute Irvington Fellowship. A. Iannello holds a Special Fellow Award from the Leukemia and Lymphoma Society. E. Fessler was supported by the Sofie-Wallner-Preis and the Dr. Ernst und Anita Bauer-Stiftung. This work was supported by NIH P01 CA080111 (R.A. Weinberg), U54 CA163109 (R.A. Weinberg), R01 CA093678 (D.H. Raulet), and R01 AI084880 (M.J. Pittet); the Breast Cancer Research Foundation (R.A. Weinberg); and the Ludwig Center for Molecular Oncology (R.A. Weinberg).

The costs of publication of this article were defrayed in part by the payment of page charges. This article must therefore be hereby marked *advertisement* in accordance with 18 U.S.C. Section 1734 solely to indicate this fact.

Received September 24, 2015; revised March 21, 2016; accepted April 4, 2016; published OnlineFirst April 12, 2016.

REFERENCES

1. Fidler IJ. The pathogenesis of cancer metastasis: the 'seed and soil' hypothesis revisited. Nat Rev Cancer 2003;3:453–8.
2. Wyckoff JB, Wang Y, Lin EY, Li JF, Goswami S, Stanley ER, et al. Direct visualization of macrophage-assisted tumor cell intravasation in mammary tumors. Cancer Res 2007;67:2649–56.
3. Coussens LM, Werb Z. Inflammation and cancer. Nature 2002;420:860–7.
4. de Visser KE, Eichten A, Coussens LM. Paradoxical roles of the immune system during cancer development. Nat Rev Cancer 2006;6:24–37.
5. Mantovani A, Allavena P, Sica A, Balkwill F. Cancer-related inflammation. Nature 2008;454:436–44.
6. Trinchieri G. Cancer and inflammation: an old intuition with rapidly evolving new concepts. Annu Rev Immunol 2012;30:677–706.
7. Welch DR, Schissel DJ, Howrey RP, Aeed PA. Tumor-elicited polymorphonuclear cells, in contrast to "normal" circulating polymorphonuclear cells, stimulate invasive and metastatic potentials of rat mammary adenocarcinoma cells. Proc Natl Acad Sci U S A 1989;86:5859–63.
8. Fridlender ZG, Albelda SM. Tumor-associated neutrophils: friend or foe? Carcinogenesis 2012;33:949–55.
9. Fridlender ZG, Sun J, Kim S, Kapoor V, Cheng G, Ling L, et al. Polarization of tumor-associated neutrophil phenotype by TGF-beta: "N1" versus "N2" TAN. Cancer Cell 2009;16:183–94.
10. Galdiero MR, Bonavita E, Barajon I, Garlanda C, Mantovani A, Jaillon S. Tumor associated macrophages and neutrophils in cancer. Immunobiology 2013;218:1402–10.
11. Granot Z, Henke E, Comen EA, King TA, Norton L, Benezra R. Tumor entrained neutrophils inhibit seeding in the premetastatic lung. Cancer Cell 2011;20:300–14.
12. Kowanetz M, Wu X, Lee J, Tan M, Hagenbeek T, Qu X, et al. Granulocyte-colony stimulating factor promotes lung metastasis through mobilization of $Ly6G^+Ly6C^+$ granulocytes. Proc Natl Acad Sci U S A 2010;107:21248–55.
13. Shojaei F, Wu X, Malik AK, Zhong C, Baldwin ME, Schanz S, et al. Tumor refractoriness to anti-VEGF treatment is mediated by $CD11b^+Gr1^+$ myeloid cells. Nat Biotechnol 2007;25:911–20.
14. Shojaei F, Wu X, Qu X, Kowanetz M, Yu L, Tan M, et al. G-CSF-initiated myeloid cell mobilization and angiogenesis mediate tumor refractoriness to anti-VEGF therapy in mouse models. Proc Natl Acad Sci U S A 2009;106:6742–7.
15. Sionov RV, Fridlender ZG, Granot Z. The multifaceted roles neutrophils play in the tumor microenvironment. Cancer Microenviron 2015;8:125–58.
16. Scapini P, Lapinet-Vera JA, Gasperini S, Calzetti F, Bazzoni F, Cassatella MA. The neutrophil as a cellular source of chemokines. Immunol Rev 2000;177:195–203.
17. Nozawa H, Chiu C, Hanahan D. Infiltrating neutrophils mediate the initial angiogenic switch in a mouse model of multistage carcinogenesis. Proc Natl Acad Sci U S A 2006;103:12493–8.
18. Brinckerhoff CE, Matrisian LM. Matrix metalloproteinases: a tail of a frog that became a prince. Nat Rev Mol Cell Biol 2002;3:207–14.
19. Egeblad M, Werb Z. New functions for the matrix metalloproteinases in cancer progression. Nat Rev Cancer 2002;2:161–74.
20. Ardi VC, Kupriyanova TA, Deryugina EI, Quigley JP. Human neutrophils uniquely release TIMP-free MMP-9 to provide a potent catalytic stimulator of angiogenesis. Proc Natl Acad Sci U S A 2007;104:20262–7.
21. Kessenbrock K, Plaks V, Werb Z. Matrix metalloproteinases: regulators of the tumor microenvironment. Cell 2010;141:52–67.
22. Mason SD, Joyce JA. Proteolytic networks in cancer. Trends Cell Biol 2011;21:228–37.
23. Acuff HB, Carter KJ, Fingleton B, Gorden DL, Matrisian LM. Matrix metalloproteinase-9 from bone marrow-derived cells contributes to survival but not growth of tumor cells in the lung microenvironment. Cancer Res 2006;66:259–66.
24. Hiratsuka S, Nakamura K, Iwai S, Murakami M, Itoh T, Kijima H, et al. MMP9 induction by vascular endothelial growth factor receptor-1 is involved in lung-specific metastasis. Cancer Cell 2002;2:289–300.

Published OnlineFirst April 12, 2016; DOI: 10.1158/2159-8290.CD-15-1157

25. Casbon AJ, Reynaud D, Park C, Khuc E, Gan DD, Schepers K, et al. Invasive breast cancer reprograms early myeloid differentiation in the bone marrow to generate immunosuppressive neutrophils. Proc Natl Acad Sci U S A 2015;112:E566–75.
26. Joyce JA, Pollard JW. Microenvironmental regulation of metastasis. Nat Rev Cancer 2009;9:239–52.
27. Almand B, Clark JI, Nikitina E, van Beynen J, English NR, Knight SC, et al. Increased production of immature myeloid cells in cancer patients: a mechanism of immunosuppression in cancer. J Immunol 2001;166:678–89.
28. Yang L, DeBusk LM, Fukuda K, Fingleton B, Green-Jarvis B, Shyr Y, et al. Expansion of myeloid immune suppressor Gr^+CD11b^+ cells in tumor-bearing host directly promotes tumor angiogenesis. Cancer Cell 2004;6:409–21.
29. Atzpodien J, Reitz M. Peripheral blood neutrophils as independent immunologic predictor of response and long-term survival upon immunotherapy in metastatic renal-cell carcinoma. Cancer Biother Radiopharm 2008;23:129–34.
30. Joshita S, Nakazawa K, Sugiyama Y, Kamijo A, Matsubayashi K, Miyabayashi H, et al. Granulocyte-colony stimulating factor-producing pancreatic adenosquamous carcinoma showing aggressive clinical course. Intern Med 2009;48:687–91.
31. Aslakson CJ, Miller FR. Selective events in the metastatic process defined by analysis of the sequential dissemination of subpopulations of a mouse mammary tumor. Cancer Res 1992;52:1399–405.
32. Rak JW, McEachern D, Miller FR. Sequential alteration of peanut agglutinin binding-glycoprotein expression during progression of murine mammary neoplasia. Br J Cancer 1992;65:641–8.
33. Yan HH, Pickup M, Pang Y, Gorska AE, Li Z, Chytil A, et al. $Gr\text{-}1^+CD11b^+$ myeloid cells tip the balance of immune protection to tumor promotion in the premetastatic lung. Cancer Res 2010;70:6139–49.
34. Cortez-Retamozo V, Etzrodt M, Newton A, Rauch PJ, Chudnovskiy A, Berger C, et al. Origins of tumor-associated macrophages and neutrophils. Proc Natl Acad Sci U S A 2012;109:2491–6.
35. Morris VL, Tuck AB, Wilson SM, Percy D, Chambers AF. Tumor progression and metastasis in murine D2 hyperplastic alveolar nodule mammary tumor cell lines. Clin Exp Metastasis 1993;11:103–12.
36. Shibue T, Weinberg RA. Integrin beta1-focal adhesion kinase signaling directs the proliferation of metastatic cancer cells disseminated in the lungs. Proc Natl Acad Sci U S A 2009;106:10290–5.
37. Daley JM, Thomay AA, Connolly MD, Reichner JS, Albina JE. Use of Ly6G-specific monoclonal antibody to deplete neutrophils in mice. J Leukoc Biol 2008;83:64–70.
38. Shibue T, Brooks MW, Inan MF, Reinhardt F, Weinberg RA. The outgrowth of micrometastases is enabled by the formation of filopodium-like protrusions. Cancer Discov 2012;2:706–21.
39. Barlozzari T, Reynolds CW, Herberman RB. In vivo role of natural killer cells: involvement of large granular lymphocytes in the clearance of tumor cells in anti-asialo GM1-treated rats. J Immunol 1983;131:1024–7.
40. Riccardi C, Santoni A, Barlozzari T, Puccetti P, Herberman RB. In vivo natural reactivity of mice against tumor cells. Int J Cancer 1980;25:475–86.
41. Kasai M, Yoneda T, Habu S, Maruyama Y, Okumura K, Tokunaga T. In vivo effect of anti-asialo GM1 antibody on natural killer activity. Nature 1981;291:334–5.
42. Kiessling R, Klein E, Pross H, Wigzell H. "Natural" killer cells in the mouse. II. Cytotoxic cells with specificity for mouse Moloney leukemia cells. Characteristics of the killer cell. Eur J Immunol 1975;5:117–21.
43. Fernandez NC, Treiner E, Vance RE, Jamieson AM, Lemieux S, Raulet DH. A subset of natural killer cells achieves self-tolerance without expressing inhibitory receptors specific for self-MHC molecules. Blood 2005;105:4416–23.
44. Kim S, Poursine-Laurent J, Truscott SM, Lybarger L, Song YJ, Yang L, et al. Licensing of natural killer cells by host major histocompatibility complex class I molecules. Nature 2005;436:709–13.
45. Labelle M, Hynes RO. The initial hours of metastasis: the importance of cooperative host-tumor cell interactions during hematogenous dissemination. Cancer Discov 2012;2:1091–9.
46. Vu TH, Shipley JM, Bergers G, Berger JE, Helms JA, Hanahan D, et al. MMP-9/gelatinase B is a key regulator of growth plate angiogenesis and apoptosis of hypertrophic chondrocytes. Cell 1998;93:411–22.
47. Chen MB, Whisler JA, Jeon JS, Kamm RD. Mechanisms of tumor cell extravasation in an in vitro microvascular network platform. Integr Biol (Camb) 2013;5:1262–71.
48. Erler JT, Bennewith KL, Cox TR, Lang G, Bird D, Koong A, et al. Hypoxia-induced lysyl oxidase is a critical mediator of bone marrow cell recruitment to form the premetastatic niche. Cancer Cell 2009;15:35–44.
49. Hiratsuka S, Watanabe A, Aburatani H, Maru Y. Tumour-mediated upregulation of chemoattractants and recruitment of myeloid cells predetermines lung metastasis. Nat Cell Biol 2006;8:1369–75.
50. Kaplan RN, Riba RD, Zacharoulis S, Bramley AH, Vincent L, Costa C, et al. VEGFR1-positive haematopoietic bone marrow progenitors initiate the pre-metastatic niche. Nature 2005;438:820–7.
51. Lu X, Kang Y. Chemokine (C-C motif) ligand 2 engages $CCR2^+$ stromal cells of monocytic origin to promote breast cancer metastasis to lung and bone. J Biol Chem 2009;284:29087–96.
52. Qian BZ, Li J, Zhang H, Kitamura T, Zhang J, Campion LR, et al. CCL2 recruits inflammatory monocytes to facilitate breast-tumour metastasis. Nature 2011;475:222–5.
53. Wolf MJ, Hoos A, Bauer J, Boettcher S, Knust M, Weber A, et al. Endothelial CCR2 signaling induced by colon carcinoma cells enables extravasation via the JAK2-Stat5 and p38MAPK pathway. Cancer Cell 2012;22:91–105.
54. Labelle M, Begum S, Hynes RO. Platelets guide the formation of early metastatic niches. Proc Natl Acad Sci U S A 2014;111:E3053–61.
55. Elkabets M, Ribeiro VS, Dinarello CA, Ostrand-Rosenberg S, Di Santo JP, Apte RN, et al. IL-1beta regulates a novel myeloid-derived suppressor cell subset that impairs NK cell development and function. Eur J Immunol 2010;40:3347–57.
56. Hoechst B, Voigtlaender T, Ormandy L, Gamrekelashvili J, Zhao F, Wedemeyer H, et al. Myeloid derived suppressor cells inhibit natural killer cells in patients with hepatocellular carcinoma via the NKp30 receptor. Hepatology 2009;50:799–807.
57. Liu C, Yu S, Kappes J, Wang J, Grizzle WE, Zinn KR, et al. Expansion of spleen myeloid suppressor cells represses NK cell cytotoxicity in tumor-bearing host. Blood 2007;109:4336–42.
58. Mundy-Bosse BL, Lesinski GB, Jaime-Ramirez AC, Benninger K, Khan M, Kuppusamy P, et al. Myeloid-derived suppressor cell inhibition of the IFN response in tumor-bearing mice. Cancer Res 2011;71:5101–10.
59. Gabrilovich DI, Nagaraj S. Myeloid-derived suppressor cells as regulators of the immune system. Nat Rev Immunol 2009;9:162–74.
60. Gabrilovich DI, Ostrand-Rosenberg S, Bronte V. Coordinated regulation of myeloid cells by tumours. Nat Rev Immunol 2012;12:253–68.
61. Bergers G, Brekken R, McMahon G, Vu TH, Itoh T, Tamaki K, et al. Matrix metalloproteinase-9 triggers the angiogenic switch during carcinogenesis. Nat Cell Biol 2000;2:737–44.
62. Lee S, Jilani SM, Nikolova GV, Carpizo D, Iruela-Arispe ML. Processing of VEGF-A by matrix metalloproteinases regulates bioavailability and vascular patterning in tumors. J Cell Biol 2005;169:681–91.
63. An X, Ding PR, Li YH, Wang FH, Shi YX, Wang ZQ, et al. Elevated neutrophil to lymphocyte ratio predicts survival in advanced pancreatic cancer. Biomarkers 2010;15:516–22.
64. Cho H, Hur HW, Kim SW, Kim SH, Kim JH, Kim YT, et al. Pre-treatment neutrophil to lymphocyte ratio is elevated in epithelial ovarian cancer and predicts survival after treatment. Cancer Immunol Immunother 2009;58:15–23.
65. Liu H, Liu G, Bao Q, Sun W, Bao H, Bi L, et al. The baseline ratio of neutrophils to lymphocytes is associated with patient prognosis in rectal carcinoma. J Gastrointest Cancer 2010;41:116–20.
66. Teramukai S, Kitano T, Kishida Y, Kawahara M, Kubota K, Komuta K, et al. Pretreatment neutrophil count as an independent prognostic factor in advanced non-small-cell lung cancer: an analysis of Japan Multinational Trial Organisation LC00–03. Eur J Cancer 2009;45:1950–8.

Published OnlineFirst April 12, 2016; DOI: 10.1158/2159-8290.CD-15-1157

67. Ubukata H, Motohashi G, Tabuchi T, Nagata H, Konishi S, Tabuchi T. Evaluations of interferon-gamma/interleukin-4 ratio and neutrophil/lymphocyte ratio as prognostic indicators in gastric cancer patients. J Surg Oncol 2010;102:742–7.
68. Granger JM, Kontoyiannis DP. Etiology and outcome of extreme leukocytosis in 758 nonhematologic cancer patients: a retrospective, single-institution study. Cancer 2009;115:3919–23.
69. Hasegawa S, Suda T, Negi K, Hattori Y. Lung large cell carcinoma producing granulocyte-colony-stimulating factor. Ann Thorac Surg 2007;83:308–10.
70. Hirasawa K, Kitamura T, Oka T, Matsushita H. Bladder tumor producing granulocyte colony-stimulating factor and parathyroid hormone related protein. J Urol 2002;167:2130.
71. Mabuchi S, Matsumoto Y, Morii E, Morishige K, Kimura T. The first 2 cases of granulocyte colony-stimulating factor producing adenocarcinoma of the uterine cervix. Int J Gynecol Pathol 2010;29:483–7.
72. Yamamoto S, Takashima S, Ogawa H, Kuroda T, Yamamoto M, Takeda A, et al. Granulocyte-colony-stimulating-factor-producing hepatocellular carcinoma. J Gastroenterol 1999;34:640–4.
73. Crawford J, Ozer H, Stoller R, Johnson D, Lyman G, Tabbara I, et al. Reduction by granulocyte colony-stimulating factor of fever and neutropenia induced by chemotherapy in patients with small-cell lung cancer. N Engl J Med 1991;325:164–70.
74. Galkina E, Thatte J, Dabak V, Williams MB, Ley K, Braciale TJ. Preferential migration of effector CD8$^+$ T cells into the interstitium of the normal lung. J Clin Invest 2005;115:3473–83.

Published OnlineFirst April 12, 2016; DOI: 10.1158/2159-8290.CD-15-1157

AACR American Association for Cancer Research

CANCER DISCOVERY

Neutrophils Suppress Intraluminal NK Cell–Mediated Tumor Cell Clearance and Enhance Extravasation of Disseminated Carcinoma Cells

Asaf Spiegel, Mary W. Brooks, Samin Houshyar, et al.

Cancer Discov 2016;6:630-649. Published OnlineFirst April 12, 2016.